Journal of Hydrology 513 (2014) 28–44

Contents lists available at ScienceDirect

Journal of Hydrology

journal homepage: www.elsevier.com/locate/jhydrol

Stream filtration induced by pumping in a confined, unconfined or leaky aquifer bounded by two parallel streams or by a stream and an impervious stratum

Ching-Sheng Huang [a], Wen-Sheng Lin [b], Hund-Der Yeh [a,*]

[a] Institute of Environmental Engineering, National Chiao Tung University, Hsinchu, Taiwan
[b] Hydrotech Research Institute, National Taiwan University, Taipei, Taiwan

ARTICLE INFO

Article history:
Received 28 October 2013
Received in revised form 4 March 2014
Accepted 15 March 2014
Available online 25 March 2014
This manuscript was handled by Peter K. Kitanidis, Editor-in-Chief, with the assistance of Philippe Negrel, Associate Editor

Keywords:
Stream depletion rate (*SDR*)
Robin boundary condition
Double-integral transform
Laplace transform
Padé approximation
Monte Carlo simulation

SUMMARY

A mathematical model is developed for describing three-dimensional groundwater flow induced by a fully-penetrating vertical well in aquifers between two parallel streams. A general equation is adopted to represent the top boundary condition which is applicable to either a confined, unconfined or leaky aquifer. The Robin (third-type) boundary condition is employed to represent the low-permeability streambeds. The Laplace-domain head solution of the model is derived by the double-integral and Laplace transforms. The Laplace-domain solution for a stream depletion rate (*SDR*) describing filtration from the streams is developed based on Darcy's law and the head solution and inverted to the time-domain result by the Crump method. In addition, the time-domain solution of *SDR* for the confined aquifer is developed analytically after taking the inverse Laplace transform and the time-domain solutions of *SDR* for the leaky and unconfined aquifers are developed using the Padé approximation. Both approximate solutions of *SDR* are expressed in terms of simple series and give fairly good match with the Laplace-domain *SDR* solution and measured data from a field experiment in New Zealand. The uncertainties in *SDR* predictions for the aquifers are assessed by performing the sensitivity analysis and Monte Carlo simulation. With the aid of the time-domain solutions, we have found that the effect of the vertical groundwater flow on the temporal *SDR* for a leaky aquifer is dominated by two lumped parameters: $\kappa = K_v x_0^2/(K_h D^2)$ and $\kappa' = K'D/(B'K_v)$ where D is the aquifer thickness, x_0 is a distance between the well and nearer stream, K_h and K_v are the aquifer horizontal and vertical hydraulic conductivities, respectively, and K' and B' are the aquitard hydraulic conductivity and thickness, respectively. When $\kappa < 10$, neglecting the vertical flow underestimates the *SDR*. When $\kappa \geqslant 10$, the effect of vertical flow is negligible. When $\kappa' \leqslant 10^{-4}$, the aquitard can be regarded as impermeable, and the leaky aquifer behaves as a confined one.

1. Introduction

Well pumping near a stream causes water filtration from the stream. The well could be vertical, horizontal, or vertical with laterals at the well bottom. The ratio of the filtration rate to the pumping rate is defined as a stream depletion rate (*SDR*). During the pumping period, *SDR* increases from zero to a constant value which could be equal to or less than unity. When *SDR* is zero, the filtration has not happened and the pumping has not affected the stream. *SDR* starts to increase with time when the drawdown cone reaches the stream. When *SDR* is unity, the stream filtration is at a rate which equals the pumping rate. The steady-state *SDR* is less than unity in the presence of additional recharge sources from such as an aquifer, stream, or/and long-term rainfall.

An analytical approach is commonly used to estimate *SDR* for problems involving stream water management and water rights. A variety of analytical and semi-analytical models associated with the prediction of temporal *SDR* have been proposed and categorized according to different aquifer types, well types and stream treatments. Most existing models consider a vertical well to fully penetrate an aquifer, implying that groundwater flow within the aquifer is two-dimensional (2-D). In addition, the stream is commonly treated as a boundary in the models or its effect is modeled as a source term in the governing equations of the models.

If a stream is assumed to fully penetrate an aquifer, it forms a boundary with the aquifer. Theis solution (1941) expressed in terms of the well function might be the first solution describing

* Corresponding author. Address: 300 Institute of Environmental Engineering, National Chiao Tung University, 1001 University Road, Hsinchu, Taiwan. Tel.: +886 3 5731910; fax: +886 3 5725958.
E-mail address: hdyeh@mail.nctu.edu.tw (H.-D. Yeh).

http://dx.doi.org/10.1016/j.jhydrol.2014.03.039
0022-1694/

a temporal distribution of *SDR*. In the solution development, the stream is considered as the Dirichlet (first-type) boundary condition, and image well theory is used to develop the solution. Therefore, Theis solution (1941) did not account for the effect of the low-permeability streambed on temporal *SDR*. Glover and Balmer (1954) reduced Theis solution (1941) to a complementary error function for conciseness. Swamee et al. (2000) further developed a closed-form approximate expression for Theis solution (1941). Hantush (1965) treated a stream as the Robin (third-type) boundary and derived an analytical solution accounting for the low-permeability streambed effect. The solutions mentioned above neglect the effect of streambed storage on temporal *SDR*. Recently, Sun and Zhan (2007) derived an analytical solution considering two parallel constant-head streams and the effects of the streambed's storage and permeability. Intaraprasong and Zhan (2009) further derived an analytical solution with considering the effect of a variable stage stream.

A stream may be regarded as a source term in the governing equation of groundwater flow. The term is in terms of the Dirac delta function, implying that the stream has a zero width. Those solutions considering the source term are applicable to the groundwater problem in the presence of a low-permeability streambed. On the other hand, the source term represents a fully-penetrating stream effect with neglecting the vertical flow component (Sun and Zhan, 2007). Hunt solution (1999) might be the first analytical solution derived by treating the stream as a line source and was shown to be exactly the same as Hantush solution (1965) according to Sun and Zhan (2007). Chen and Yin (2004) extended Hunt solution (1999) by considering water exchange between a stream and an aquifer prior to pumping. Recently, Zlotnik and Tartakovsky (2008) treated a stream as a line source and presented an analytical solution for a leaky aquifer with leakage at the bottom of the aquifer.

In order to account for the effect of a stream width, some researchers divided an aquifer into three zones with different governing flow equations. The middle zone has a width equaling the stream width, and a source term is in its governing flow equation and distributed over the whole spatial domain. A fully-penetrating well is in one of the side zones and treated as a sink term in its governing equation. The other side zone considers no source or sink term in the governing flow equation. Those three governing equations are coupled via the continuities of head and flux at the interfaces between the middle zone and side zones (Zlotnik and Huang, 1999). Butler et al. (2001) used this approach to derive a semi-analytical solution for a confined aquifer and addressed the effect of the stream width on *SDR*. Fox et al. (2002) considered the same model as Butler et al. (2001) but derived an analytical solution in the time domain.

A multiple-layer aquifer system is commonly represented by a quasi three-dimensional (3-D) flow model in which the flow in the aquifer is horizontal and in the aquitard is vertical. The aquifer system may be classified into a leaky aquifer or two-layer aquifer system. The leaky aquifer consists of a main aquifer and an aquitard either on the top or at the bottom. The groundwater flow in the aquitard is assumed to be vertical due to the low hydraulic conductivity. Hunt (2003) developed an analytical solution for head and stream filtration in the leaky aquifer overlain by a thin aquitard with a free surface. The stream with a zero width is treated as a source term in the governing equation for the underlying aquifer. Hunt (2008) also considered the same aquifer but a finite width stream. The aquifer extends infinitely along the stream and is bounded by the no-flow boundaries in the direction perpendicular to the stream. He developed a semi-analytical solution for hydraulic head and stream filtration. Butler et al. (2007) derived a semi-analytical solution describing hydraulic head and stream filtration for the leaky aquifer with an underlying aquitard. The two-layer aquifer system has two main aquifers with an aquitard embedded in the middle. Hunt (2009) developed a semi-analytical solution for such an aquifer system. The stream is treated as a source term of a zero width, and a vertical well fully penetrates the upper aquifer. Recently, Ward and Lough (2011) considered the same situation but the well was installed at the lower aquifer. They derived a semi-analytical solution in the Fourier and Laplace domain for hydraulic head and in the Laplace domain for stream filtration.

Some researchers developed an analytical solution in predicting *SDR* induced by a slanted well, horizontal well or radial collector well. The solution takes account of the vertical component of groundwater flow even in a confined aquifer. Based on a 3-D groundwater flow equation, Tsou et al. (2010) derived an analytical solution for the temporal *SDR* induced by a slanted well in a confined aquifer. The slanted well can behave as a horizontal or vertical one by adjusting the orientation and inclination of the well. They found that the water flow filtration from a fully-penetrating stream toward a horizontal well parallel to the stream will reach steady state quickly. Huang et al. (2011) used a 3-D groundwater flow equation along with a simplified free surface equation representing the upper boundary of an unconfined aquifer and developed an analytical solution for the temporal *SDR* induced by a horizontal well. Their solution can investigate the effect of specific yield on *SDR*. These two solutions consider the stream as the Dirichlet boundary in the absence of a low-permeability streambed. Recently, Huang et al. (2012a) considered the streambed as the Robin boundary and presented an analytical solution to describe hydraulic head and temporal *SDR* induced by a radial collector well in an unconfined aquifer. They reported that the largest drawdown at the water table occurs right at the well center at the beginning of the pumping and moves landward when the filtration occurs.

Some semi-analytical solutions to a problem involving a horizontal well in a leaky aquifer underlying a water reservoir were also presented. The reservoir is of infinite extent in the horizontal direction and treated as a constant-head boundary at the top of the aquifer. Zhan and Park (2003) presented a semi-analytical solution for such a situation. The aquifer directly connects the overlying reservoir without a low-permeability aquitard in between. Sun and Zhan (2006) developed a semi-analytical solution for the same situation but considered the effects of aquitard storage and permeability.

Some researchers considered a wedge-shaped confined or unconfined aquifer and treated the adjacent stream as the Dirichlet boundary condition. Yeh et al. (2008) developed an analytical solution for the hydraulic head and *SDR* induced by a fully-penetrating vertical well in the wedge-shaped confined aquifer with an arbitrary angle. Singh (2009) also developed an analytical solution for *SDR* but for a right-angled confined aquifer. Sedghi et al. (2009) presented a semi-analytical solution for 3-D groundwater flow in the wedge-shaped confined or unconfined aquifer with a partially-penetrating vertical well. Other studies considered a triangle-shaped aquifer for simulating a delta aquifer surrounded by a stream. Asadi-Aghbolaghi and Seyyedian (2010) derived a closed-form solution describing a 2-D steady-state head distribution induced by a fully-penetrating vertical well in the triangle-shaped confined aquifer.

The solutions mentioned above are summarized in Tables 1 and 2. In Table 1, all of the solutions dealing with the 2-D flow problem induced by a fully-penetrating vertical well are categorized based on aquifer types and stream treatments. In Table 2, the solutions involving the quasi 3-D flow or 3-D flow are categorized based on aquifer categories, well types, and stream treatments. In these two tables, the superscripts *a* and *b* stand for the presentation of the time-domain solution and Laplace-domain solution, respectively.

Table 1
Classification of the solutions involving 2-D flow induced by a fully-penetrating vertical well.

References	Aquifer type	Stream treatment
Theis (1941)[a]	Confined aquifer	Dirichlet boundary condition
Glover and Balmer (1954)[a]	Confined aquifer	Dirichlet boundary condition
Hantush (1965)[a]	Confined aquifer	Robin boundary condition
Hunt (1999)[a]	Confined aquifer	Source term of a zero-width stream
Swamee et al. (2000)[a]	Confined aquifer	Dirichlet boundary condition
Butler et al. (2001)[b]	Confined aquifer	Source term of a finite-width stream
Fox et al. (2002)[a]	Confined aquifer	Source term of a finite-width stream
Chen and Yin (2004)[a]	Confined aquifer	Source term of a zero-width stream considering water exchange between the stream and aquifer
Sun and Zhan (2007)[a]	Confined aquifer divided into three zones, two side zones of which are regarded as low-permeability streambeds	Two parallel streams treated as Dirichlet boundary conditions
Zlotnik and Tartakovsky (2008)[a]	Leaky aquifer	Source term of a zero-width stream
Yeh et al. (2008)[a]	Wedge-shaped confined aquifer	Dirichlet boundary condition
Singh (2009)[a]	Right-angled confined aquifer	Dirichlet boundary condition
Intaraprasong and Zhan (2009)[a]	Confined aquifer divided into two zones, one of which is regarded as a low-permeability streambed	Dirichlet boundary condition with a variable stream stage
Asadi-Aghbolaghi and Seyyedian (2010)[a]	Triangle-shaped confined aquifer	Dirichlet boundary condition

[a] Time-domain solution.
[b] Laplace-domain solution.

Table 2
Classification of the solutions involving quasi 3-D and 3-D groundwater flow.

References	Aquifer type	Well type	Stream treatment
Quasi 3-D flow			
Hunt (2003)[a]	Leaky aquifer with an overlying aquitard having a free surface	Fully-penetrating vertical well	Source term of a zero-width stream
Butler et al. (2007)[b]	Leaky aquifer with an underlying aquitard	Fully-penetrating vertical well	Source term of a finite-width stream
Hunt (2008)[b]	The same aquifer as Hunt (2003)	Fully-penetrating vertical well	Source term of a finite-width stream
Hunt (2009)[b]	Two-layer aquifer system	Fully-penetrating vertical well in the upper aquifer	Source term of a zero-width stream in a governing equation for the top aquifer
Ward and Lough (2011)[b]	Two-layer aquifer system	Fully-penetrating vertical well in the lower aquifer	Source term of a zero-width stream in a governing equation for the top aquifer
3-D flow			
Zhan and Park (2003)[b]	Leaky aquifer underlying a water reservoir	Horizontal well	Constant-head reservoir connecting the lower aquifer without an aquitard in between
Sun and Zhan (2006)[b]	Leaky aquifer underlying a water reservoir	Horizontal well	Constant-head reservoir connecting the lower aquifer with an aquitard in between
Sedghi et al. (2009)[b]	Wedge-Shaped unconfined aquifer	Partially-penetrating vertical well	Dirichlet boundary condition
Tsou et al. (2010)[a]	Confined aquifer	Slanted well	Dirichlet boundary condition
Huang et al. (2011)[a]	Unconfined aquifer	Horizontal well	Dirichlet boundary condition
Huang et al. (2012a)[a]	Unconfined aquifer	Radial collector well	Robin boundary condition

[a] Time-domain solution.
[b] Laplace-domain solution.

The calculation efficiency of existing *SDR* solutions for an unconfined aquifer has required improvement (e.g., Huang et al., 2011, 2012a). The solutions are expressed in terms of a multiple integral, which may cause problems of time-consuming calculation and inaccurate numerical integration. For example, the recent solution developed by Huang et al. (2012a) involves an infinite series expanded by sequences and a quadruple integral consisting of three improper integrals and one finite integral. Moreover, two of the integration variables depend on the sequences which are the roots of two nonlinear equations. The application of their solution may be limited to those who are good at numerical methods for the solution calculation.

The *SDR* problem associated with 3-D groundwater flow in a leaky aquifer has not been dealt with so far. Existing *SDR* solutions consider 2-D groundwater flow and treat the leakage through an aquitard as a source term in the governing flow equation, which excludes the effect of an aquifer vertical hydraulic conductivity on *SDR*. For considering the effect, the leakage can be included in a boundary condition on the top of the aquifer (Huang et al., 2012b).

This paper develops a mathematical model for describing 3-D groundwater flow induced by pumping in a fully-penetrating vertical well in three types of aquifers bounded by two parallel streams or by a stream and an impervious stratum. A general equation is adopted to represent the top boundary condition which is applicable to either a confined, unconfined or leaky aquifer (Huang et al., 2012b). The streams with low-permeability streambeds form the Robin boundary. The head solution of the model is derived by

the double-integral transform and Laplace transform. Based on Darcy's law and the head solution, the Laplace-domain *SDR* solution is developed and inverted to closed-form time-domain results by applying the Padé approximation and inverse Laplace transform. The time-domain *SDR* solutions for the aquifers are expressed in terms of a simple series, and the accuracy is examined by means of the Laplace-domain *SDR* solution inverted numerically by Crump method (1976). The steady-state distribution of the filtration from the two streams is discussed. The effect of the vertical component of groundwater flow on temporal *SDR* for the leaky aquifer is investigated. Additionally, the temporal *SDR* predicted by the time-domain solution for the confined aquifer matches with the field *SDR* experiment given in Hunt et al. (2001). Moreover, the uncertainty in the *SDR* predictions from the time-domain solutions is assessed by performing the sensitivity analysis and Monte Carlo simulation.

2. Methodology

In this section, we first introduce the mathematical model for flow induced by a fully-penetrating vertical well in an aquifer bounded by two parallel streams and present the Laplace-domain head and *SDR* solutions of the model. The Crump method (1976) is then used to invert both Laplace-domain solutions to time-domain results. After that, a procedure based on Newton's method with appropriate initial guesses is proposed to determine the eigenvalues of the solutions. In addition, Padé approximation is applied to the Laplace-domain *SDR* solution, and the closed-form time-domain results are obtained after taking the inverse Laplace transform. Finally, the time-domain *SDR* solutions in terms of a simple series expanded by the eigenvalues for confined, leaky and unconfined aquifers are presented. The notations used in the text are summarized in Table 3.

2.1. Mathematical model

Even if the numerical simulation of *SDR* considers different types of wells, such as a vertical well with different penetration and a radial collector well with symmetrical laterals, it leads to almost the same result (e.g., Sophocleous et al., 1995; Huang et al., 2012a). We therefore consider a fully-penetrating vertical well for simplicity. In solving a problem associated with water right distributions, we consider two parallel streams (Sun and Zhan, 2007). Fig. 1(a) shows the schematic diagram of an aquifer with the well located between the parallel streams. The aquifer has a finite width W_x bounded by the two streams in x-direction and W_y bounded by two no-flow boundaries in y-direction. Streambeds 1 and 2 have a width B_1 and B_2, respectively. The well is located at (x_0, y_0). The aquifer has a thickness D in Fig. 1(b) for a confined condition, Fig. 1(c) for an unconfined condition and Fig. 1(d) for a leaky condition. The overlying aquitard has a thickness B' in Fig. 1(d).

The governing equation describing 3-D transient hydraulic head $h(x, y, z, t)$ induced by pumping in a fully-penetrating vertical well can be expressed as

$$K_h\frac{\partial^2 h}{\partial x^2}+K_h\frac{\partial^2 h}{\partial y^2}+K_v\frac{\partial^2 h}{\partial z^2}=S_s\frac{\partial h}{\partial t}+\frac{Q}{D}\delta(x-x_0)\delta(y-y_0) \tag{1}$$

where $\delta()$ is the Dirac delta function, K_h and K_v are hydraulic conductivities in the horizontal and vertical directions, respectively, S_s is specific storage, Q is a constant discharge rate, and t is the time since pumping.

The value of hydraulic head depends on the location of the reference datum, a surface of zero elevation. The datum is located at the initial potentiometric surface for confined aquifers and initial water table elevations for leaky aquifers and unconfined aquifers. The initial condition is therefore written as

$$h=0 \quad \text{at} \quad t=0 \tag{2}$$

A partially penetrating stream can be considered as full penetration if the distance from the stream to the well is larger than 1.5 times the aquifer thickness (e.g., Jacob, 1950; Todd and Mays, 2005). The parallel streams with low-permeability streambeds can be represented by the Robin boundary conditions as

$$\frac{\partial h}{\partial x}-\frac{K_1}{K_hB_1}h=0 \quad \text{at} \quad x=0 \tag{3}$$

$$\frac{\partial h}{\partial x}+\frac{K_2}{K_hB_2}h=0 \quad \text{at} \quad x=W_x \tag{4}$$

where K_1 and K_2 are the hydraulic conductivity of streambeds 1 and 2, respectively.

Table 3
Notations used in the text, their default values used in calculation, and field data of the aquifer near Doyleston in New Zealand.

Notations	Default value (unit)	Field data (unit)	Description
h	None	None	Hydraulic head
(x, y, z)	None	None	Variables of Cartesian coordinate
t	None	None	Time
(K_h, K_v)	(1, 0.1) m/day	(3.78,[a] none) m/h	Aquifer horizontal and vertical hydraulic conductivities, respectively
(S_y, S_s)	(0.1, 10^{-5} m^{-1})	(none, 10^{-4}[a] m^{-1})	Aquifer specific yield and specific storage, respectively
(D, W_x, W_y)	(20 m, 10 km, 10 km)	(20 m,[a] 1 km, 1 km)	Aquifer thickness and widths in x and y directions, respectively
(T, S)	(20 m^2/day, 2×10^{-4})	(75.6 m^2/h, 2×10^{-3})[a]	Aquifer transmissivity (K_hD) and storage coefficient (S_sD), respectively
(K', B')	(0.01 m/day, 1 m)	None	Aquitard conductivity and its thickness, respectively
(K_1, B_1)	(0.1 m/day, 1 m)	(0.0089 m/h, 1 m)[a]	Hydraulic conductivity and thickness of streambed 1, respectively
(K_2, B_2)	(0, 1 m)	(0, 1 m)	Hydraulic conductivity and thickness of streambed 2, respectively
Q	None	63[a] m^3/h	Pumping rate of a vertical well
(x_0, y_0)	(50 m, 250 m)	(55,[a] 500) m	Location of a vertical well
α_i	None	None	Roots of Eq. (11)
h_D	None	None	K_hDh/Q
(x_D, y_D, z_D, t_D)	None	None	$(x/x_0, y/x_0, z/D, K_ht/(S_sx_0^2))$
(x_{0D}, y_{0D})	(1, 5)	None	$(x_0/x_0, y_0/x_0)$
$(\kappa, \kappa', \sigma)$	(0.625, 2, 500)	None	$(K_vx_0^2/(K_hD^2), K'D/(K_vB'), S_y/S)$
(κ_1, κ_2)	(50, 0)	None	$(K_1x_0/(K_hB_1), K_2/(K_hB_2))$
(ω_x, ω_y)	(10, 10)	None	$(W_x/x_0, W_y/x_0)$
(λ_a, λ_p)	None	None	$\left(\alpha_i/\sqrt{\kappa}, \sqrt{b_1^2-4b_2}\right)$
(a_0, b_1, b_2)	None	None	Coefficients of Padé approximation defined in Eq. (23)
$\tilde{S}(x_D, \alpha_i)$	None	None	Function of x_d and α_i defined in Eq. (15d)

[a] Reported by Hunt et al. (2001).

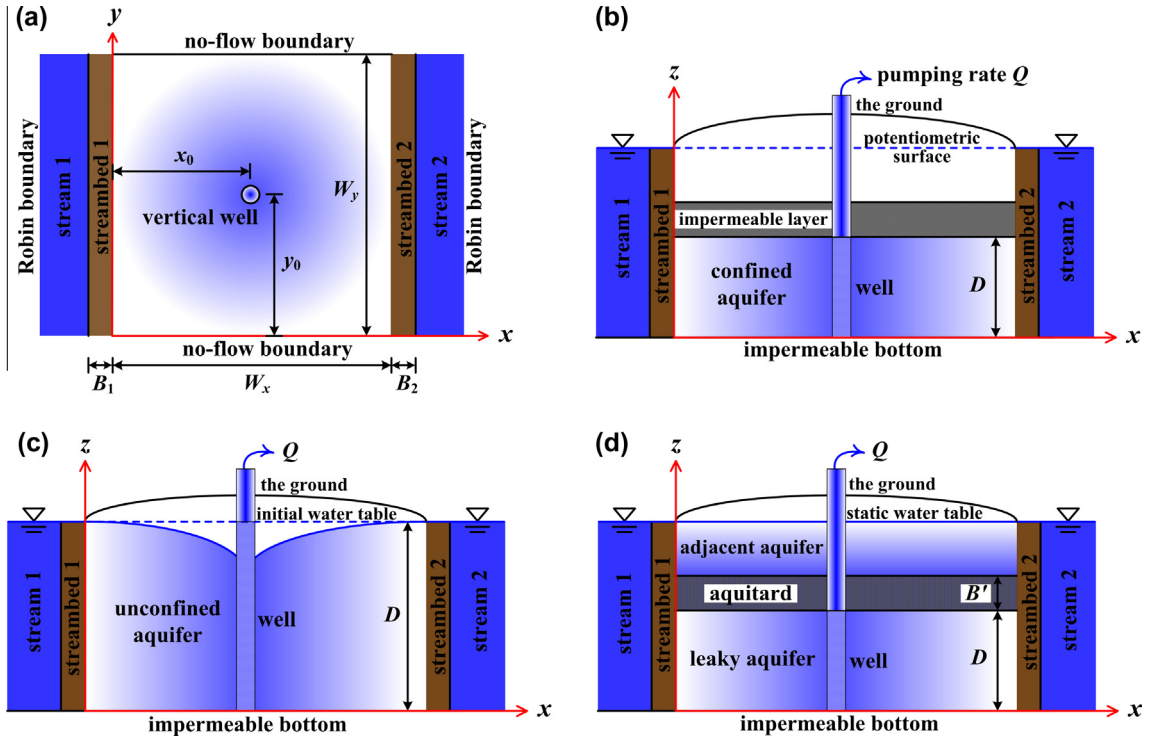

Fig. 1. Schematic diagram of a finite aquifer with a fully-penetrating vertical well bounded by two parallel streams: (a) a top view of the aquifer and a cross-section view of (b) confined, (c) unconfined and (d) leaky conditions.

Consideration of an aquifer extending infinitely or semi-infinitely leads to the *SDR* solution in terms of a multiple integral which is not integrable (e.g., Butler et al., 2007; Tsou et al., 2010; Huang et al., 2012a). In order to obtain an analytical expression for the multiple integral in the *SDR* solution of the model (Eqs. (14a) and (14b)), we consider the no-flow boundary condition at y-direction of the finite aquifer as

$$\partial h/\partial y = 0 \quad \text{at} \quad y = 0 \text{ and } y = W_y \tag{5}$$

Note that the numerical result calculated from the head solution developed based on Eq. (5) should be equal to that obtained from the solution with a remote boundary condition of $\lim_{y\to\pm\infty}\partial h/\partial y = 0$, if the width W_y is larger than the radius of influence of a pumping well.

The no-flow boundary condition is applied at the lower boundary of the aquifer and stands for an impermeable medium as

$$\partial h/\partial z = 0 \quad \text{at} \quad z = 0 \tag{6}$$

A general equation representing the top boundary condition for confined, unconfined and leaky aquifers is expressed as (Huang et al., 2012b)

$$K_v\frac{\partial h}{\partial z} + \frac{K'}{B'}h = -S_y\frac{\partial h}{\partial t} \quad \text{at} \quad z = D \tag{7}$$

where S_y is specific yield for the unconfined condition, and K' is aquitard's vertical hydraulic conductivity (aquitard's storage and horizontal hydraulic conductivity are assumed zero). Eq. (7) reduces to $K_v\,\partial h/\partial z + (K'/B')h = 0$ for the leaky condition when $S_y = 0$, $K_v\,\partial h/\partial z = -S_y\,\partial h/\partial t$ for the unconfined condition when $K' = 0$, and $\partial h/\partial z = 0$ for the confined condition when $S_y = 0$ and $K' = 0$. Note that $K_v\,\partial h/\partial z = -S_y\,\partial h/\partial t$ is a simplified equation for describing the change of the free surface in an unconfined aquifer (e.g., Neuman, 1972; Zhan and Zlotnik, 2002; Teo et al., 2003; Yeh et al., 2010).

Introduce dimensionless variables and parameters as

$$h_D = \frac{K_hD}{Q}h, \quad x_D = \frac{x}{x_0}, \quad y_D = \frac{y}{x_0}, \quad y_{0D} = \frac{y_0}{x_0}, \quad z_D = \frac{z}{D},$$

$$t_D = \frac{K_ht}{S_sx_0^2}, \quad \sigma = \frac{S_y}{S}, \quad \kappa = \frac{K_vx_0^2}{K_hD^2}, \quad \kappa' = \frac{K'D}{B'K_v},$$

$$\kappa_1 = \frac{K_1x_0}{B_1K_h}, \quad \kappa_2 = \frac{K_2x_0}{B_2K_h}, \quad \omega_x = \frac{W_x}{x_0}, \quad \omega_y = \frac{W_y}{x_0} \tag{8}$$

where $S = S_sD$, and the subscript D represents a dimensionless symbol for the variables. Based on Eq. (8), Eqs. (1)–(7) can be expressed, respectively, as

$$\frac{\partial^2h_D}{\partial x_D^2} + \frac{\partial^2h_D}{\partial y_D^2} + \kappa\frac{\partial^2h_D}{\partial z_D^2} = \frac{\partial h_D}{\partial t_D} + \delta(x_D - 1)\delta(y_D - y_{0D}) \tag{9a}$$

$$h_D = 0 \quad \text{at} \quad t_D = 0 \tag{9b}$$

$$\frac{\partial h_D}{\partial x_D} - \kappa_1h_D = 0 \quad \text{at} \quad x_D = 0 \tag{9c}$$

$$\frac{\partial h_D}{\partial x_D} + \kappa_2h_D = 0 \quad \text{at} \quad x = \omega_x \tag{9d}$$

$$\partial h_D/\partial y_D = 0 \quad \text{at} \quad y_D = 0 \text{ and } y = \omega_y \tag{9e}$$

$$\partial h_D/\partial z_D = 0 \quad \text{at} \quad z_D = 0 \tag{9f}$$

$$\frac{\partial h_D}{\partial z_D} + \kappa'h_D = -\frac{\sigma}{\kappa}\frac{\partial h_D}{\partial t_D} \quad \text{at} \quad z_D = 1 \tag{9g}$$

2.2. Laplace-domain solution for hydraulic head

The model becomes a boundary value problem in terms of z_D after taking the double-integral transform and Laplace transform.

For the detailed definition of the double-integral transform, readers can refer to Appendix A. The second-order differential operators $\partial^2/\partial x_D^2$ and $\partial^2/\partial y_D^2$ in Eq. (9a) can be converted to parameters when applying the double-integral transform (Latinopoulos, 1985, Eq. (9)). Similarly, the first-order differential operator $\partial/\partial t_D$ is converted to a parameter when applying the Laplace transform. As such, Eq. (9a) becomes an ordinary differential equation in terms of z_D as

$$\kappa\frac{d^2\bar{h}_D}{dz_D^2}-\left(p+\alpha_i^2+\beta_j^2\right)\bar{h}_D=\frac{1}{p}K_e(1,\alpha_i)\cos(y_{0D}\beta_j) \tag{10a}$$

with

$$K_e(x_D,\alpha_i)=\sqrt{2}\frac{\alpha_i\cos(\alpha_i x_D)+\kappa_1\sin(\alpha_i x_D)}{\sqrt{(\alpha_i^2+\kappa_1^2)[\omega_x+\kappa_2/(\alpha_i^2+\kappa_2^2)]+\kappa_1}} \tag{10b}$$

where $\beta_j=\pi j/\omega_y$, $j\in 1,2,\ldots\infty$, $K_e(1,\alpha_i)$ is defined by $K_e(x_D,\alpha_i)$ with $x_D=1$, p is the Laplace transform parameter, and α_i are the positive eigenvalues/roots of (Latinopoulos, 1985, Table I, aquifer type 4)

$$\tan(\omega_x\alpha_i)=\frac{\alpha_i(\kappa_1+\kappa_2)}{\alpha_i^2-\kappa_1\times\kappa_2} \tag{11}$$

The method to estimate α_i is illustrated in Section 2.3. Based on those transforms, Eqs. (9f) and (9g) respectively become

$$d\bar{h}_D/dz_D=0 \quad \text{at} \quad z_D=0 \tag{12a}$$

$$\frac{d\bar{h}_D}{dz_D}+\kappa'\bar{h}_D=-\frac{\sigma}{\kappa}p\bar{h}_D \quad \text{at} \quad z_D=1 \tag{12b}$$

Solving Eq. (10a) with Eqs. (12a) and (12b) and inverting the result by the formulas for the inverse double-integral transform (Eq. (A.3) in Appendix A) leads to the Laplace-domain head solution as

$$\bar{h}_D(x_D,y_D,z_D,p)=\frac{1}{\omega_y}\left\{\sum_{i=1}^{\infty}\left[\hat{h}(\alpha_i,0,z_D,p)+2\sum_{j=1}^{\infty}\hat{h}(\alpha_i,\beta_j,z_D,p)\cos(\beta_j y_D)\right]S(x_D,\alpha_i)\right\} \tag{13a}$$

with

$$S(x_D,\alpha_i)=2\frac{\alpha_i\cos(\alpha_i x_D)+\kappa_1\sin(\alpha_i x_D)}{\kappa_1+(\alpha_i^2+\kappa_1^2)\left[\omega_x+\kappa_2/(\alpha_i^2+\kappa_2^2)\right]} \tag{13b}$$

$$\hat{h}(\alpha_i,\beta_j,z_D,p)=\frac{V(\alpha_i,\beta_j)}{\kappa p\lambda(\alpha_i,\beta_j,p)^2}\left(\frac{[(\sigma/\kappa)p+\kappa']\cosh[\lambda(\alpha_i,\beta_j,p)z_D]}{\eta(\alpha_i,\beta_j,p)}-1\right) \tag{13c}$$

$$V(\alpha_i,\beta_j)=\cos(\beta_j y_{0D})(\alpha_i\cos\alpha_i+\kappa_1\sin\alpha_i) \tag{13d}$$

$$\lambda(\alpha_i,\beta_j,p)=\sqrt{\left(p+\alpha_i^2+\beta_j^2\right)/\kappa} \tag{13e}$$

$$\eta(\alpha_i,\beta_j,p)=(\sigma/\kappa)p\cosh[\lambda(\alpha_i,\beta_j,p)]+\kappa'\cosh[\lambda(\alpha_i,\beta_j,p)]+\lambda(\alpha_i,\beta_j,p)\sinh[\lambda(\alpha_i,\beta_j,p)] \tag{13f}$$

The solution contains one simple series expanded by α_i and one double series expanded by α_i and j.

2.3. Laplace-domain solution for SDR

Based on Darcy's law and Eq. (13) (i.e., including Eqs. (13a)–(13f)), the solution describing Laplace-domain *SDR* from streams 1 and 2 can be written, respectively, as

$$\overline{SDR}_1(p)=-\int_{z=0}^{z=1}\int_{y=0}^{y=\omega_y}\frac{\partial\bar{h}_D}{\partial x_D}dy_D dz_D \quad \text{at} \quad x_D=0 \tag{14a}$$

$$\overline{SDR}_2(p)=\int_{z=0}^{z=1}\int_{y=0}^{y=\omega_y}\frac{\partial\bar{h}_D}{\partial x_D}dy_D dz_D \quad \text{at} \quad x=\omega_x \tag{14b}$$

Substituting Eq. (13a) into Eqs. (14a) and (14b) and integrating the results with respect to y_D and z_D yields, respectively,

$$\overline{SDR}_1(p)=-\sum_{i=1}^{\infty}\tilde{h}(\alpha_i,0,p)\tilde{S}(0,\alpha_i) \tag{15a}$$

and

$$\overline{SDR}_2(p)=\sum_{i=1}^{\infty}\tilde{h}(\alpha_i,0,p)\tilde{S}(\omega_x,\alpha_i) \tag{15b}$$

with

$$\tilde{h}(\alpha_i,\beta_j,p)=\frac{[(\sigma/\kappa)p+\kappa']\sinh[\lambda(\alpha_i,\beta_j,p)]}{\kappa p\lambda(\alpha_i,\beta_j,p)^3\eta(\alpha_i,\beta_j,p)}-\frac{1}{\kappa p\lambda(\alpha_i,\beta_j,p)^2} \tag{15c}$$

$$\tilde{S}(x_D,\alpha_i)=2\frac{[\alpha_i\cos\alpha_i+\kappa_1\sin\alpha_i]\left[-\alpha_i^2\sin(\alpha_i x_D)+\kappa_1\alpha_i\cos(\alpha_i x_D)\right]}{\kappa_1+(\alpha_i^2+\kappa_1^2)\left[\omega_x+\kappa_2/(\alpha_i^2+\kappa_2^2)\right]} \tag{15d}$$

Notice that the double integral in Eq. (14a), (14b) is integrable because of the introduction of Eq. (5), and the double series in Eq. (13a) reduces to zero because of the integration to y_D in Eq. (14a) or (14b). The *SDR* solution is therefore in terms of the simple series expanded by α_i, which improves the efficiency in calculation and works only for the case of the no-flow boundary conditions defined in Eq. (5).

Eq. (15) (i.e., including Eqs. (15a)–(15d)) is now a general solution in the Laplace domain for confined, leaky, and unconfined aquifers. When $\sigma=0$ and $\kappa'=0$ (i.e., $S_y=0$ and $K'=0$), the first term on the right-head side (RHS) of Eq. (15c) equals zero and then Eq. (15) is the Laplace-domain *SDR* solution for the confined aquifer. In addition, Eq. (15) becomes the Laplace-domain *SDR* solution for the leaky aquifer if $\sigma=0$ (i.e., $S_y=0$) and for the unconfined aquifer if $\kappa'=0$ (i.e., $K'=0$).

2.4. Numerical inversion

Both Laplace-domain solutions, Eqs. (13) and (15), can be inverted numerically by Crump method (1976) which involves calculation of an infinite series as

$$f(t_D)=\frac{\exp(at_D)}{T_p}\left\{\frac{\bar{f}(a)}{2}+\sum_{k=1}^{\infty}\mathrm{Re}\left[\bar{f}\left(a+\frac{i\pi k}{T_p}\right)\cos\left(\frac{\pi k t_D}{T_p}\right)\right]-\mathrm{Im}\left[\bar{f}\left(a+\frac{i\pi k}{T_p}\right)\sin\left(\frac{\pi k t_D}{T_p}\right)\right]\right\} \tag{16}$$

where $i=\sqrt{-1}$, $f(t_D)$ is a time-domain result of $\bar{f}(p)$, $\bar{f}(p)$ represents the Laplace-domain solution defined by either Eq. (13) or (15), T_p is an interesting dimensionless time domain as $0\leqslant t_D\leqslant T_p$, Re and Im represent the real and imaginary parts of a complex number, respectively, $a=\phi-(\ln E)/2T_p$ with E, an error tolerance, suggested as 10^{-8} and ϕ, representing the real part of a leading pole for $\bar{f}(p)$ or equaling zero for a function without any pole. The leading pole is zero for both Laplace-domain solutions.

2.5. Numerical evaluation for eigenvalues α_i

The eigenvalues α_i can be determined from Eq. (11) as consecutive positive roots obtained using Newton's method with appropriate initial guesses. Based on the left hand side (LHS) and RHS functions of the equation, the initial guesses for the roots

can be determined analytically. The eigenvalues α_i are in fact located at the intersection points of the LHS and RHS functions of the equation and near the vertical asymptotes of the periodical function $\tan(\omega_x\alpha_i)$. The locations of the asymptotes depend on the conditions that $\kappa_2 \neq 0$ and $\kappa_2 = 0$. When $\kappa_2 = 0$, the initial guesses for α_i are considered as $(2i-1)\pi/(2\omega_x) - \delta$ where δ is a small value, say 10^{-8}, in preventing the initial guesses located right at the vertical asymptotes. When $\kappa_2 \neq 0$, there is one additional vertical asymptote located at $\alpha_i = \sqrt{\kappa_1\kappa_2}$ originated from letting the denominator of the RHS function of Eq. (11) be zero. The initial guesses for α_i are chosen as $(2i-1)\pi/(2\omega_x) + \delta$ when $(2i-1)\pi/(2\omega_x) < \sqrt{\kappa_1\kappa_2}$ and as $(2i-1)\pi/(2\omega_x) - \delta$ when $(2i-1)\pi/(2\omega_x) > \sqrt{\kappa_1\kappa_2}$.

The roots of Eq. (11) depend on the specific permeabilities of the streambeds, κ_1 and κ_2. When $\kappa_1 \to \infty$ and $\kappa_2 \to \infty$ (i.e., $B_1 = 0$ and $B_2 = 0$), both streambeds do not exist, indicating that the streams directly connect the aquifer and can be considered as a constant-head boundary. Under such a condition, Eq. (11) reduces to $\tan(\omega_x\alpha_i) = 0$ and the roots α_i can be derived analytically as $\alpha_i = i\pi/\omega_x$. On the other hand, streambed 1 does not exist and streambed 2 is totally impermeable when $\kappa_1 \to \infty$ and $\kappa_2 = 0$ (i.e., $B_1 = 0$ and $K_2 = 0$). Stream 1 can be regarded as a constant head boundary while stream 2 becomes a no-flow one. Under this circumstance, Eq. (11) becomes $\tan(\omega_x\alpha_i) \to \infty$ and the roots α_i are equal to $(2i-1)\pi/(2\omega_x)$.

2.6. Time-domain solution for SDR in confined aquifer

Substituting $\sigma = 0$ and $\kappa' = 0$ into Eq. (15) and taking the inverse Laplace transform to the result yields the time-domain *SDR* solution for the confined aquifer as

$$SDR_1(t_D) = -\sum_{i=1}^{\infty} f(\alpha_i, t_D)\tilde{S}(0, \alpha_i) \tag{17a}$$

$$SDR_2(t_D) = \sum_{i=1}^{\infty} f(\alpha_i, t_D)\tilde{S}(\omega_x, \alpha_i) \tag{17b}$$

with

$$f(\alpha_i, t_D) = -\frac{1}{\alpha_i^2}\left[1 - \exp(-\alpha_i^2 t_D)\right] \tag{17c}$$

Eq. (17a) or (17b) gives almost the same numerical result of *SDR* as Glover and Balmer solution (1954) if the well is close to the nearby stream to avoid the filtration from the other one.

2.7. Padé approximation

If $\sigma \neq 0$ or $\kappa' \neq 0$, the inverse Laplace transform for Eq. (15) may not be tractable due to the complexity of the first RHS term (i.e., represented by $\bar{F}(p)$) in Eq. (15c). We therefore adopt Padé approximation to develop a closed-form expression for the inverse Laplace transform. Based on Padé approximation, $\bar{F}(p)$ can be approximated using a quotient of two polynomials denoted as (Gerald and Wheatley, 1994)

$$\bar{F}(p) \cong \frac{a_0 + a_1 p + a_2 p^2 + \cdots + a_n p^n}{1 + b_1 p + b_2 p^2 + \cdots + b_m p^m} \tag{18}$$

where a_n and b_m depend on the coefficients c_i of Maclaurin series of $\bar{F}(p)$ as

$$\bar{F}(p) \cong c_0 + c_1 p + c_2 p^2 + \cdots + c_N p^N \tag{19}$$

where $c_i = \bar{F}^{(i)}(0)/(i!)$ and $N = n + m$. The determination of a_n and b_m is discussed in Section 2.8.

2.8. Time-domain solution of SDR for unconfined aquifer

When $\sigma \neq 0$ and $\kappa' = 0$, a quotient of a zero-order polynomial over a second-order one is used to approximate $\bar{F}(p)$ as

$$\bar{F}(p) \cong \frac{a_0}{1 + b_1 p + b_2 p^2} \tag{20}$$

The Maclaurin series of $\bar{F}(p)$ with $\kappa' = 0$ can be written as

$$\bar{F}(p) \cong c_0 + c_1 p + c_2 p^2 \tag{21}$$

where the c_0, c_1, and c_2 are defined by Eqs. (25d), (25e), and (25f), respectively. The coefficients a_0, b_1 and b_2 are determined by letting the RHS functions of Eqs. (20) and (21) be the same and then by rearranging the result as

$$(c_0 - a_0) + (c_1 + c_0 b_1)p + (c_2 + c_1 b_1 + c_0 b_2)p^2 + (c_2 b_1 + c_1 b_2)p^3 + c_2 b_2 p^4 = 0 \tag{22}$$

Setting the first, second and third terms on the LHS of Eq. (22) to be zero leads to three equations. Solving the equations simultaneously, one can obtain

$$\begin{aligned} a_0 &= c_0 \\ b_1 &= -c_1/c_0 \\ b_2 &= (c_1^2 - c_0 \times c_2)/c_0^2 \end{aligned} \tag{23}$$

The inverse Laplace transform for Eq. (20) is

$$F(t_D) = -\frac{a_0}{\lambda_p}\left[\exp\left(-\frac{b_1 + \lambda_p}{2b_2}t_D\right) - \exp\left(-\frac{b_1 - \lambda_p}{2b_2}t_D\right)\right] \tag{24}$$

where $\lambda_p = \sqrt{b_1^2 - 4b_2}$. The RHS function of Eq. (24) increases with time from zero to a certain value and then decreases toward zero. This function is capable of describing the temporal *SDR* distribution for unconfined aquifers as discussed in Section 3.1.

The inverse Laplace transform for the second RHS term in Eq. (15c) is equivalent to Eq. (17c). Based on Eqs. (17) and (24), the time-domain *SDR* solution for the unconfined aquifer is written as

$$SDR_1(t_D) = -\sum_{i=1}^{\infty} f(\alpha_i, t_D)\tilde{S}(0, \alpha_i) \tag{25a}$$

$$SDR_2(t_D) = \sum_{i=1}^{\infty} f(\alpha_i, t_D)\tilde{S}(\omega_x, \alpha_i) \tag{25b}$$

with

$$f(\alpha_i, t_D) = -\frac{c_0}{\lambda_p}\left[\exp\left(-\frac{b_1 + \lambda_p}{2b_2}t_D\right) - \exp\left(-\frac{b_1 - \lambda_p}{2b_2}t_D\right)\right] - \frac{1}{\alpha_i^2}\left[1 - \exp\left(-\alpha_i^2 t_D\right)\right] \tag{25c}$$

$$c_0 = \sigma/\alpha_i^4 \tag{25d}$$

$$c_1 = -\frac{\sigma}{\alpha_i^6}\left(2 + \frac{\sigma\lambda_a}{\tanh\lambda_a}\right) \tag{25e}$$

$$c_2 = \frac{\sigma}{2\alpha_i^8}\left\{6 + \sigma\lambda_a\left[\frac{5}{\tanh\lambda_a} + \frac{\lambda_a}{(\sinh\lambda_a)^2} + \frac{2\sigma\lambda_a}{(\tanh\lambda_a)^2}\right]\right\} \tag{25f}$$

where $\lambda_a = \alpha_i/\sqrt{\kappa}$.

2.9. Time-domain solution of SDR for leaky aquifer

When $\sigma = 0$ and $\kappa' \neq 0$, $\bar{F}(p)$ can be expressed as $\bar{F}(p) = \bar{G}(p)/p$ where $\bar{G}(p)$ is a function of p. We adopt a quotient of a zero-order polynomial over a first-order one in approximating $\bar{G}(p)$ as

$$\bar{G}(p) \cong \frac{a_0}{1+b_1 p} \tag{26}$$

The Maclaurin series of $\bar{G}(p)$ can be written as

$$\bar{G}(p) \cong c_0 + c_1 p \tag{27}$$

where the c_0 and c_1 are defined by Eqs. (29d) and (29e), respectively. Similar to the procedure taken for the unconfined aquifer as described above, the a_0 and b_1 in Eq. (26) are defined in Eq. (23). The inverse Laplace transform for Eq. (26) is

$$G(t_D) = \frac{a_0}{b_1} \exp\left(-\frac{t_D}{b_1}\right) \tag{28}$$

The inverse Laplace transform for $\bar{F}(p)$ is obtained by integrating Eq. (28) with respect to t_D from 0 to t_D based on the convolution theory. With that, the time-domain *SDR* solution for the leaky aquifer is then obtained as

$$SDR_1(t_D) = -\sum_{i=1}^{\infty} f(\alpha_i, t_D)\tilde{S}(0, \alpha_i) \tag{29a}$$

$$SDR_2(t_D) = \sum_{i=1}^{\infty} f(\alpha_i, t_D)\tilde{S}(\omega_x, \alpha_i) \tag{29b}$$

with

$$f(\alpha_i, t_D) = c_0\left[1 - \exp\left(-\frac{c_0}{c_1}t_D\right)\right] - \frac{1}{\alpha_i^2}\left[1 - \exp\left(-\alpha_i^2 t_D\right)\right] \tag{29c}$$

$$c_0 = \frac{\sqrt{\kappa}\kappa' \sinh\lambda_a}{\alpha_i^3(\kappa' \cosh\lambda_a + \lambda_a \sinh\lambda_a)} \tag{29d}$$

$$c_1 = \kappa' \frac{3\kappa' \sinh(2\lambda_a) - 2\lambda_a[2 + \kappa' - 2\cosh(2\lambda_a)]}{4\kappa^2 \lambda_a^5 (\kappa' \cosh\lambda_a + \lambda_a \sinh\lambda_a)^2} \tag{29e}$$

2.10. Evaluation of uncertainty in SDR prediction

The uncertainty in *SDR* predictions associated with hydraulic parameters can be assessed by means of the sensitivity analysis and Monte Carlo simulation. The former and latter methods are introduced in Sections 2.10.1 and 2.10.2, respectively.

2.10.1. Sensitivity analysis

Sensitivity analysis is applied to evaluate the change of the *SDR* in response to the change of the parameter in the model. A dimensionless expression for the sensitivity to a specific parameter can be written as

$$S_{i,t} = P_i \frac{\partial SDR}{\partial P_i} \tag{30}$$

where the *SDR* herein is the time-domain solution defined by either Eqs. (17), (25) or (29), P_i represents the ith parameter in the solution, and $S_{i,t}$ is a normalized sensitivity coefficient at time t for the ith parameter. Eq. (30) can be discretized as

$$S_{i,t} = P_i \frac{SDR(P_i + \Delta P_i) - SDR(P_i)}{\Delta P_i} \tag{31}$$

where ΔP_i, a small increment, is set to $10^{-3}P_i$ (Huang and Yeh, 2007).

2.10.2. Monte Carlo simulation

The Monte Carlo simulation is performed to quantify uncertainty in the *SDR* predictions from the time-domain solutions. The parameters of S_s, S_y, K_h, K', K_v and K_1 are considered to be normally distributed with mean values given in the second column of Table 3. The standard deviations are 10^{-6} for S_s, 0.03 for S_y, 0.2 for K_h, 0.02 for K' and 0.06 for K_v and K_1. The realizations (or samples) of each parameter are generated by a computer-based random number generator. The simulation run for each realization is made based on the time-domain solution for a confined, unconfined or leaky aquifer. A histogram (or frequency plot) is constructed by dividing the total *SDR* predictions into an interval of 0.05 and calculating the relative frequency in each interval. The relative frequency is defined by the ratio of the number of the *SDR* predictions within the interval to the total ones. The number of the realizations for each parameter is 100. The histogram exhibits an estimated probability distribution of the *SDR* due to the variability in those parameters.

3. Results and discussion

Sources of water contributing to pumping are analyzed in Section 3.1. The accuracy of the time-domain solutions is illustrated in Section 3.2. The temporal *SDR* distribution for a narrow aquifer bounded by a stream and a no-flow boundary is displayed in Section 3.3. The distributions of the filtration from two parallel streams for the three types of aquifers are discussed in Section 3.4. The effects of κ and κ' on a temporal *SDR* for the leaky aquifer are investigated in Section 3.5. The *SDR* predicted by the time-domain solution for the confined aquifer and compared with field observation data is discussed in Section 3.6. The uncertainty in the *SDR* predictions is assessed in Section 3.7. The default values of the variables and hydraulic parameters used for calculation are listed in Table 3.

3.1. Sources contributing to pumping

Water contributing to pumping comes from various sources such as *SDR*, storage release rate (*SRR*), gravity drainage rate (*GDR*), and leakage rate (*LR*). The *SRR* in response to the compression of an aquifer matrix and the expansion of groundwater can be defined as

$$SRR(t_D) = -\int_0^1 \int_0^{\omega_y} \int_0^{\omega_x} \frac{\partial h_D}{\partial t_D} dx_D dy_D dz_D \tag{32}$$

where h is obtained by replacing $\bar{f}(p)$ in Eq. (16) with $\bar{h}_D(p)$ in Eq. (13). The *GDR* induced by the water table decline is defined as

$$GDR(t_D) = -\sigma \int_0^{\omega_y} \int_0^{\omega_x} \frac{\partial h_D}{\partial t_D} dx_D dy_D \quad \text{at} \quad z_D = 1 \tag{33}$$

The *LR* through an aquitard is defined as

$$LR(t_D) = \kappa \int_0^{\omega_y} \int_0^{\omega_x} \frac{\partial h_D}{\partial z_D} dx_D dy_D \quad \text{at} \quad z_D = 1 \tag{34}$$

The triple integral in Eq. (32) and the double integral in Eqs. (33) and (34) can be integrated analytically.

Fig. 2(a) displays the temporal distributions of the SDR_1 and *SRR* predicted by Eqs. (15a) and (32), respectively, with $\sigma = 0$ and $\kappa' = 0$ for the confined aquifer. The sum of the SDR_1 and *SRR* at any pumping time is unity, indicating that both stream filtration and storage release contribute to the well discharge. When $t_D \leqslant 0.05$, the SDR_1 is zero, and the *SRR* is unity. All of the well discharge comes from the aquifer storage. When $0.05 < t_D \leqslant 30$, the *SRR* decreases with time while the SDR_1 increases. The filtration from stream 1 starts. When $t_D > 30$, the SDR_1 is unity, and the *SRR* is zero, indicating that only the filtration contributes to the well discharge. Fig. 2(b) shows the temporal SDR_1, *SRR* and *GDR* predicted by Eqs. (15a), (32), and (33), respectively, with $\kappa' = 0$ for the unconfined aquifer. The well discharge comes from the combinations of the stream filtration, aquifer storage release and gravity drainage since the sum of the SDR_1, *SRR* and *GDR* at a fixed time is unity. The *GDR* increases

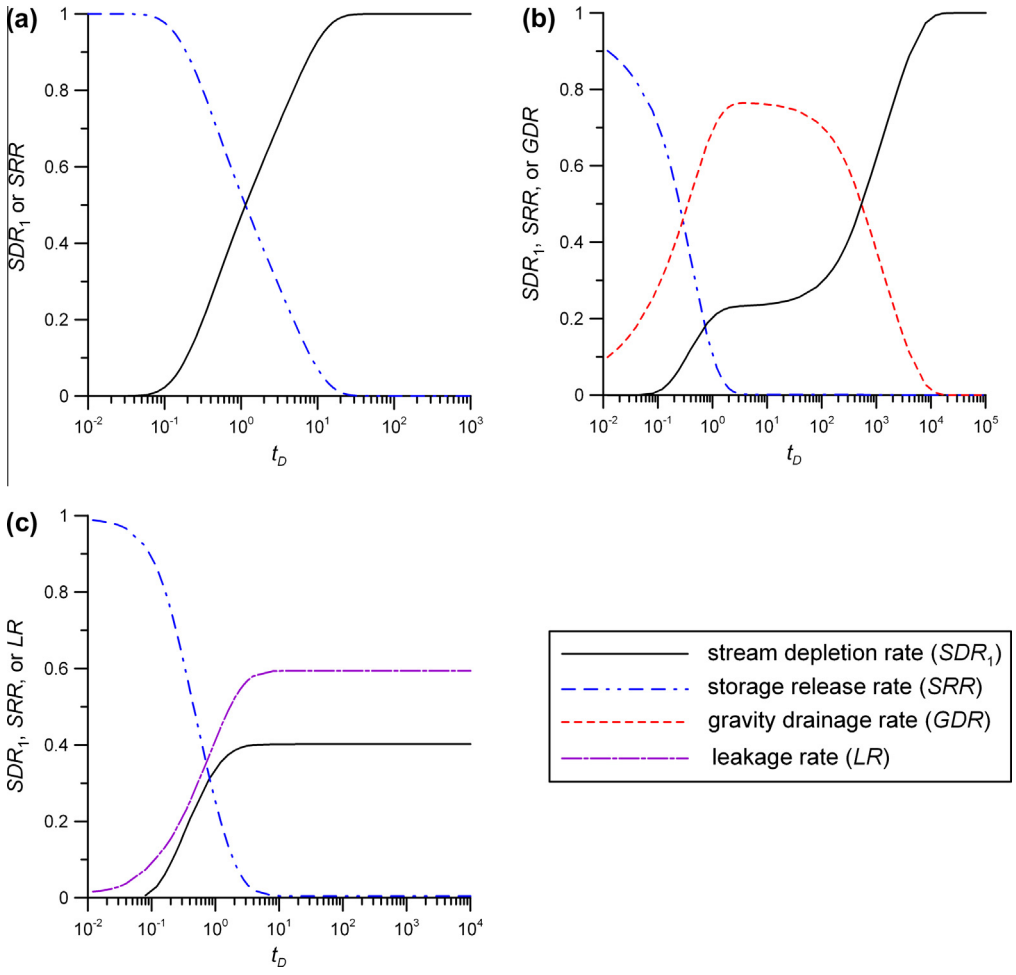

Fig. 2. Temporal distributions of the sources contributing to pumping for (a) confined, (b) unconfined and (c) leaky aquifers.

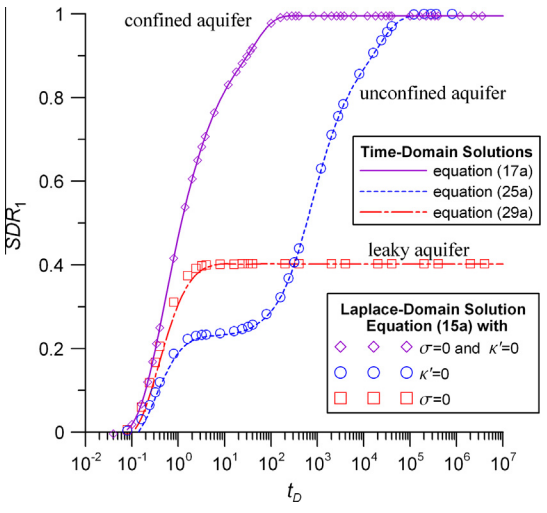

Fig. 3. Temporal *SDR* distributions predicted by both Laplace-domain solution and time-domain solution for confined, leaky and unconfined aquifers.

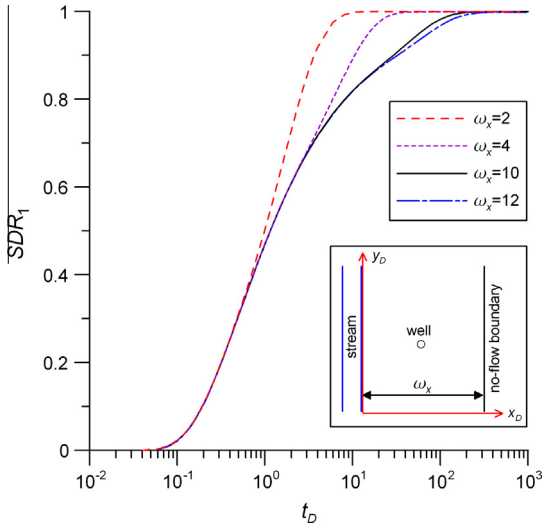

Fig. 4. Temporal *SDR* distributions predicted by the time-domain solution, Eq. (17a), for a confined aquifer bounded by a stream and the no-flow boundary for ω_x = 2, 4, 10, and 12.

initially with time, then keeps a value between 0.7 and 0.8 during the period of $2 < t_D < 100$, and finally decreases toward zero. Note that the *SRR* maintains zero during the period. The SDR_1 therefore reaches its flat stage because of the *GDR*. Furthermore, Fig. 2(c) illustrates the temporal SDR_1, *SRR* and *LR* predicted by Eqs. (15a), (32), and (34), respectively, with $\sigma = 0$ for the leaky aquifer. The sum of the SDR_1, *SRR* and *LR* is unity at any time, implying that the stream filtration, aquifer storage release, and leakage contribute to the well discharge. The *LR* varies with time and reaches

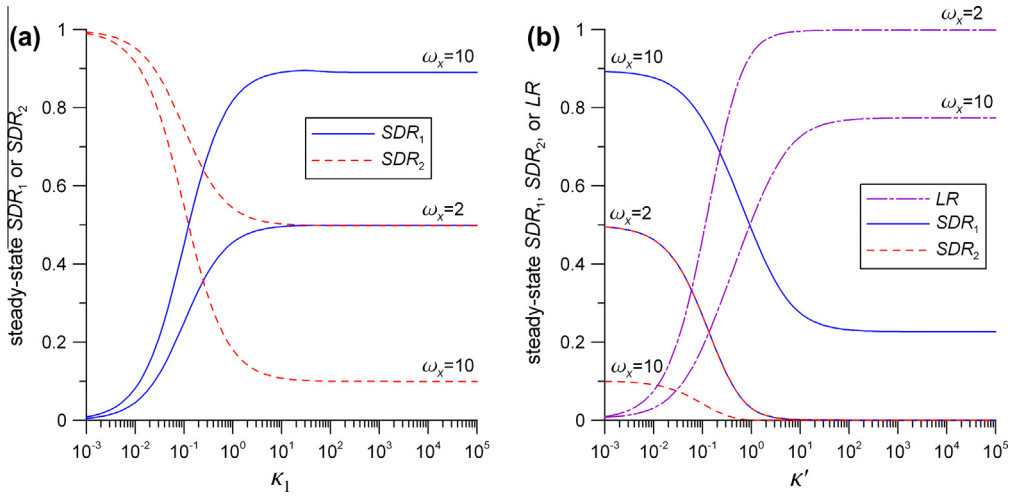

Fig. 5. Distributions of steady-state *SDR* from two parallel streams for $\omega_x = 2$ and 10 versus (a) κ_1 to a confined or unconfined aquifer and (b) κ' to a leaky aquifer.

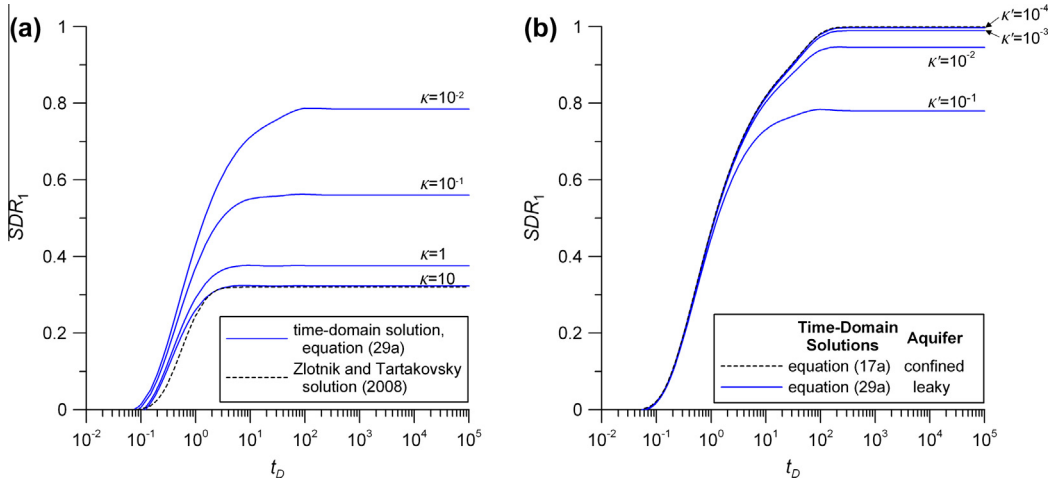

Fig. 6. Temporal *SDR* distributions predicted by the time-domain solution, Eq. (29a), for a leaky aquifer with (a) $\kappa = 10^{-2}$, 10^{-1}, 1 and 10 and (b) $\kappa' = 10^{-1}$, 10^{-2}, 10^{-3} and 10^{-4}.

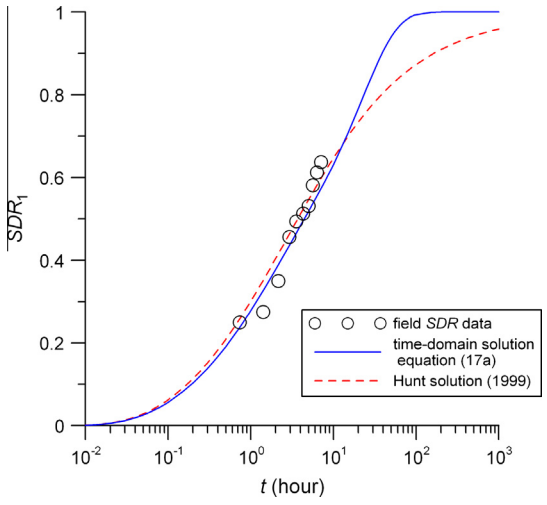

Fig. 7. Comparison of the temporal *SDR* predicted by the time-domain solution, Eq. (17a), and Hunt solution (1999) with field data taken from the field experiment conducted by Hunt et al. (2001).

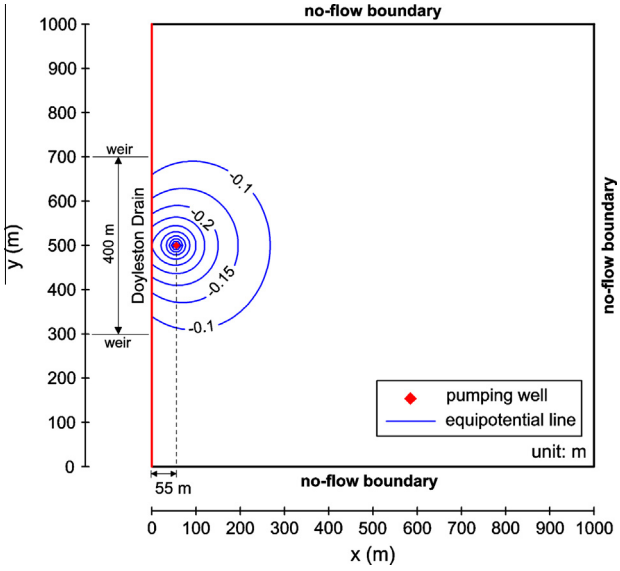

Fig. 8. The hydraulic head distribution predicted by the Laplace-domain solution, Eq. (13), for the aquifer adjacent to Doyleston Drain when $t = 10$ h.

steady state of $LR = 0.6$ when $t_D = 10$, which makes the steady-state SDR_1 less than unity.

3.2. Temporal SDR predicted by the Laplace-domain and time-domain solutions

In order to assess the accuracy of the time-domain solutions developed based on Padé approximation, their predictions are compared with those of the Laplace-domain *SDR* solution inverted by the Crump method (1976). The hydraulic parameters are considered in the range of 10^{-4}~10^{4} m/day for K_h, 10^{-7}~10^{-2} m^{-1} for S_s, 10–100 m for D, and 0.01–0.3 for S_y. The value of K_v ranges between $0.1K_h$ and $0.33K_h$ (Freeze and Cherry, 1979). The value of κ' ranges from 10^{-4} to 100. The values of $K_1/(K_hB_1)$ and $K_2/(K_hB_2)$ are chosen in the range of 10^{-5} to 1 m^{-1}. The time-domain solutions are valid when the parameter values fall in those ranges. Fig. 3 shows the predicted temporal *SDR* distributions for the three-types of aquifers. The time-domain solution, Eq. (29a), for the leaky aquifer is compared with the Laplace-domain solution, Eq. (15a) with $\sigma = 0$, while the time-domain solution, Eq. (25a), for the unconfined aquifer is also compared with Eq. (15a) with $\kappa' = 0$. Both time-domain solutions give accurate results of the temporal *SDR* for the leaky and unconfined aquifers. On the other hand, the time-domain solution, Eq. (17a), for the confined aquifer is compared with Eq. (15a) with $\sigma = 0$ and $\kappa' = 0$ and performs the same *SDR* distribution.

3.3. Effect of no-flow boundary on temporal SDR

Miller et al. (2007) indicates that a narrow aquifer bounded by a stream and the no-flow boundary leads to more *SDR* than that an extending semi-infinitely aquifer without the no-flow boundary. The present model is also applicable to the problem involving the narrow aquifer. Eq. (3) represents a stream boundary when $K_1 \neq 0$ and the no-flow boundary when $K_1 = 0$. Similarly, Eq. (4) behaves as a stream boundary when $K_2 \neq 0$ and the no-flow boundary when $K_2 = 0$. The narrow confined aquifer shown in Fig. 4 is taken for example. The temporal distributions of the *SDR* predicted by the time-domain solution for the confined aquifer when $\omega_x = 2$, 4, 10 and 12 are illustrated in Fig. 4. The aquifer with a smaller ω_x has a larger *SDR* at a fixed time, indicating that the temporal *SDR* is affected significantly by the no-flow boundary close to the well as concluded by Miller et al. (2007).

3.4. Distributions of steady-state SDR from two streams

The time-domain solutions can be used to determine the quantity of water from two parallel streams. Consider the steady-state *SDR* from the streams for confined, unconfined, and leaky aquifers. The solution describing the steady-state *SDR* for the confined aquifer can be obtained by neglecting the exponential term of time in Eq. (17c). Notice that the steady-state *SDR* solution for the unconfined aquifer is the same as that for the confined one. The steady-

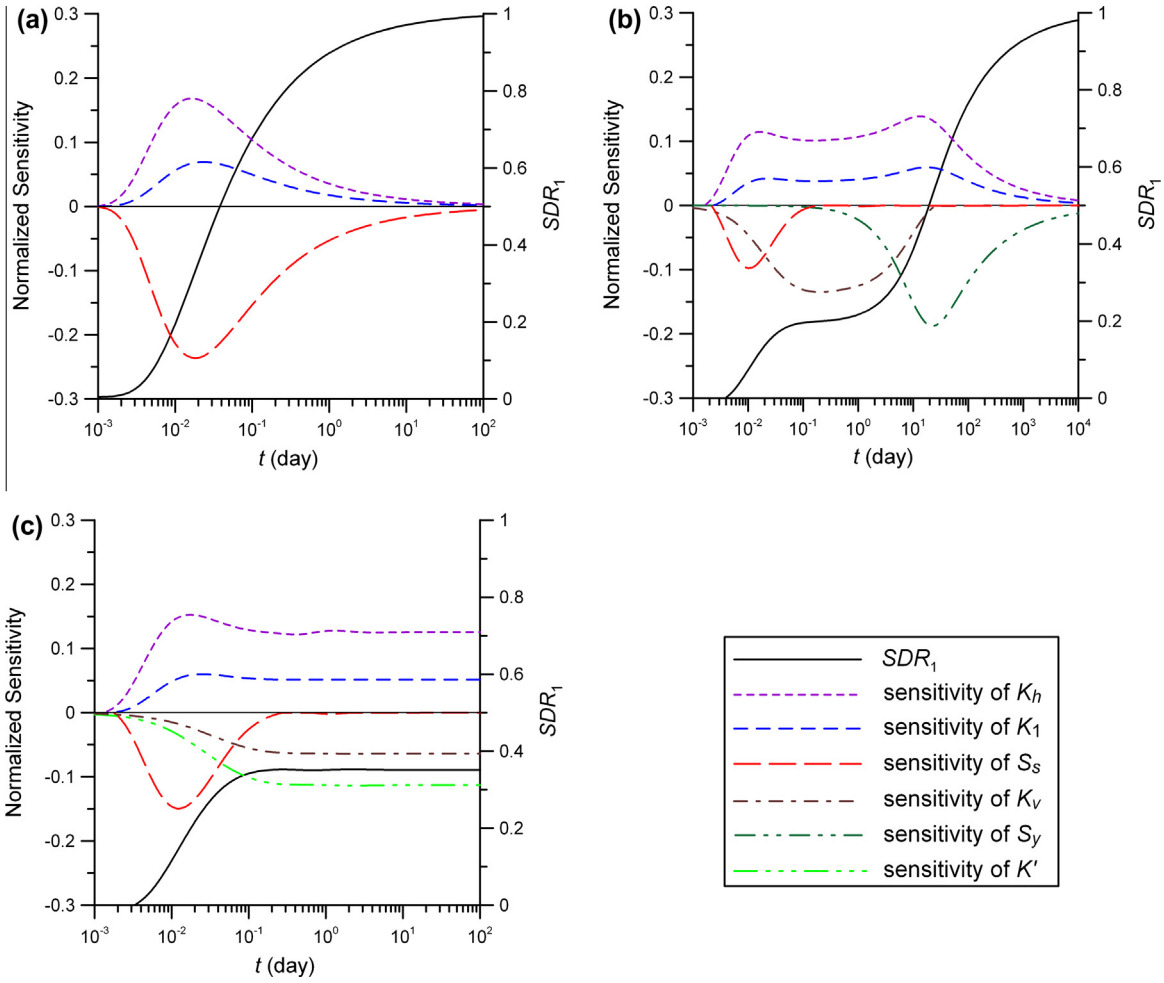

Fig. 9. Temporal distributions of the normalized sensitivity coefficients of the *SDR* to (a) K_h, K_1 and S_s for a confined aquifer (b) K_h, K_v, K_1, S_s and S_y for an unconfined aquifer and (c) K_h, K_v, K_1, K' and S_s for a leaky aquifer.

state solution for the leaky aquifer can also be derived by neglecting the exponential terms of time in Eq. (29c). Fig. 5(a) shows the steady-state SDR_1 and SDR_2 calculated by Eqs. (17a) and (17b), respectively, versus κ_1 when $\omega_x = 2$ and 10 (i.e., $x_0 = 250$ and 50 m based on $W_x = 500$ m). Streambed 2 is considered as a part of the aquifer because of $K_2 = K_h$. The sum of the SDR_1 and SDR_2 for any value of κ_1 is unity, indicating that the filtration from both streams contributes to well discharge. When $\kappa_1 > 20$, both SDR_1 and SDR_2 are 0.5 if the well is installed at the middle of the aquifer (i.e., $\omega_x = 2$). Under such a circumstance, there is no effect of the streambed permeability on *SDR*. When $\kappa_1 < 20$, SDR_2 is larger than SDR_1, reflecting that the filtration from stream 2 contributes to well discharge more than that from stream 1 due to the low permeability of streambed 1. It is worth noting that, when $\kappa_1 < 10^{-1}$, SDR_2 is greater than SDR_1 even if the well is located at $x_0 = 50$ m (i.e., $\omega_x = 10$) which is indeed very close to stream 1. Obviously, the filtration from stream 2 contributes most of the pumped water.

The steady-state SDR_1 and SDR_2 predicted by Eqs. (29a) and (29b), respectively, versus κ' with $\omega_x = 2$ and 10 for the leaky aquifer is illustrated in Fig. 5(b). The steady-state *LR* defined by Eq. (34) is taken into account for exploring water sources. The hydraulic conductivities of both streambeds are considered to be the same as that of the aquifer. The sum of the SDR_1, SDR_2 and *LR* for any value of κ' is unity. The filtration from both streams and the leakage from the adjacent aquifer therefore contribute to well discharge. For the case of $\omega_x = 2$, the well lies at the center of the aquifer, which makes the aquifer system symmetrical. Both SDR_1 and SDR_2 thus have exactly the same result due to the symmetry. The *LR* equals unity, and both SDR_1 and SDR_2 are zero when $\kappa' > 10$, indicating that all of the well discharge comes from the leakage. For the case of $\omega_x = 10$, the sum of the SDR_1 and *LR* contributes to 90–100% of the well discharge, and the SDR_2 contributes to the rest. Most of the discharge comes from the leakage when $\kappa' > 2$ and the filtration from stream 1 when $\kappa' < 2$.

3.5. Effects of κ and κ' on temporal SDR for leaky aquifer

Zlotnik and Tartakovsky (2008) developed an analytical *SDR* solution for 2-D horizontal flow in a leaky aquifer. The leakage is considered as a source term in the groundwater flow equation. If the vertical flow in the aquifer is significant, the leakage should be treated as the boundary condition, expressed as Eq. (7) with $S_y = 0$, rather than the source term contained in the governing equation. The effect of the vertical flow on a temporal *SDR* can be evaluated by the difference in *SDR* predicted by the Zlotnik and Tartakovsky solution and present time-domain solution, Eq. (29a), with $\kappa = 0.01$, 0.1, 1, and 10 shown in Fig. 6(a). Note that their solution does not have the parameter K_v due to neglecting the vertical flow and has a lumped parameter defined, in our notation, as

$$B_d^2 = \frac{B' K_h D}{K' x_0^2} \tag{35}$$

which equals the definition of $1/(\kappa\kappa')$. The value of $1/(\kappa\kappa')$ is 0.8 according to Table 3 for each *SDR* curve predicted by the present time-domain in Fig. 6(a). The figure indicates that Zlotnik and Tartakovsky solution (2008) underestimates the *SDR* when $\kappa < 10$ and

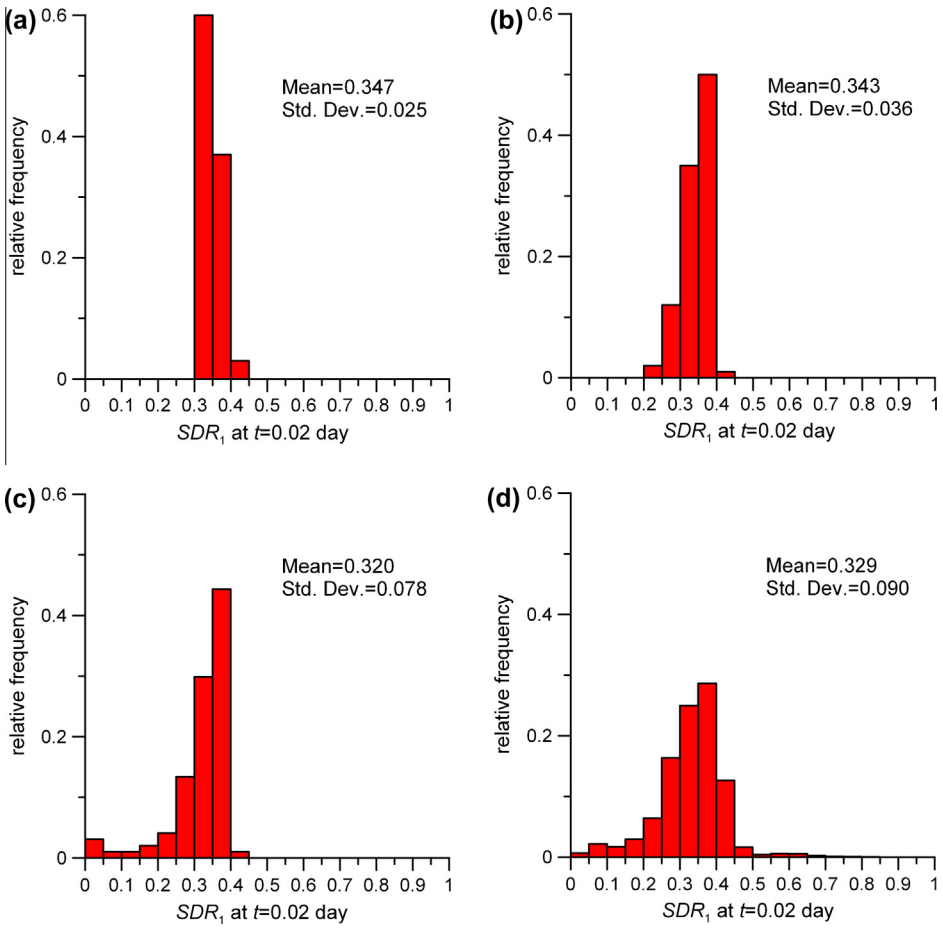

Fig. 10. Histograms of the *SDR* at $t = 0.02$ day for a confined aquifer with random variables of (a) S_s, (b) K_h, (c) K_1 and (d) S_s, K_h and K_1.

the difference in the *SDR* predicted by both solutions increases as κ decreases. When $\kappa = 10$, the present solution agrees well with Zlotnik and Tartakovsky solution (2008), implying that the vertical flow is ignorable. The slight difference in the period of $t_D < 2$ is due to the use of Padé approximation in developing the time-domain solution as discussed in Section 3.2.

Fig. 6(b) reveals that the smaller κ' leads to the larger *SDR* for the leaky aquifer. This is because, under the same well discharge, the lower permeability of the aquitard causes less leakage replenishment from the adjacent aquifer and thus more filtration from the stream. When $\kappa' = 10^{-4}$, the temporal *SDR* for the leaky aquifer is very close to that for the confined one, indicating that the aquitard can be regarded as an impermeable medium and the leaky aquifer behaves as the confined one when $\kappa' \leqslant 10^{-4}$.

3.6. Comparison with field data

Hunt et al. (2001) conducted a stream depletion field experiment by using a vertical well near Doyleston Drain, which is located about 40 km south of Christchurch in New Zealand. The drain has 2.5 m width and penetrates 1.0 m deep into the aquifer. The aquifer consists of unconsolidated sand and gravel with an average thickness of 20 m. The aquifer is confined by a less permeable material. The distance between the well and the drain is 55 m which is larger than 1.5 times the aquifer thickness. The effect of the vertical groundwater flow near the drain is therefore negligible. The well has a constant pumping rate of 63 m^3/h for 10 h. Four observation wells were installed at 5 m, 29 m, 80 m, and 88 m, respectively, away from the drain. Field *SDR* values were measured by two V-notched weirs installed in the drain. One weir was located 200 m upstream from the well while the other was located 200 m downstream from the well. Thus, in 400 m reach between those two weirs, a large amount of filtration through the edge of the drain is provided. The difference in the stream flow rates measured from those two weirs is the filtration rate from the drain to the aquifer. Field *SDR* data were then estimated by dividing the flow rate difference by the pumping rate as shown in Fig. 7.

In the field experiment, Hunt solution (1999) was used to estimate the hydraulic parameters of the aquifer and streambed near Doyleston Drain. The aquifer transmissivity and storage coefficient are 75.6 m^2/h and 2×10^{-3}, respectively, based on the temporal drawdown observed in the field which agrees well with that predicted by Hunt drawdown solution (1999). The hydraulic conductivity and specific storage are therefore 3.78 m/h and 10^{-4} m^{-1}, respectively, based on 20 m aquifer thickness. Moreover, the streambed leakage parameter is determined as 0.357 by matching the field *SDR* data with the prediction by Hunt *SDR* solution (1999) and defined as $2DK_1/B_1$ according to Sun and Zhan (2007). The ratio of the streambed hydraulic conductivity to its thickness (K_1/B_1) is thus 0.0089 h^{-1} for $D = 20$ m. The hydraulic parameters and aquifer data mentioned above are summarized in Table 3.

Fig. 7 shows the estimated *SDR* reported by Hunt et al. (2001) and the temporal *SDR* predicted by the time-domain solution for the confined aquifer with the hydraulic parameters mentioned above. Hunt *SDR* solution (1999) is taken for comparison. The aquifer width for both W_x and W_y is set to 1000 m. Both solutions agree well with the field *SDR* data. As shown in Fig. 7, the difference in *SDR* after $t = 10$ h can be attributed to the fact that the present model considers the aquifer with the no-flow condition at the finite boundary in x direction but Hunt model considers an infinite aquifer. Fig. 8 illustrates the spatial distribution of the corresponding hydraulic head predicted by Eq. (13) with $S_y = 0$ and $\kappa = 0$ when

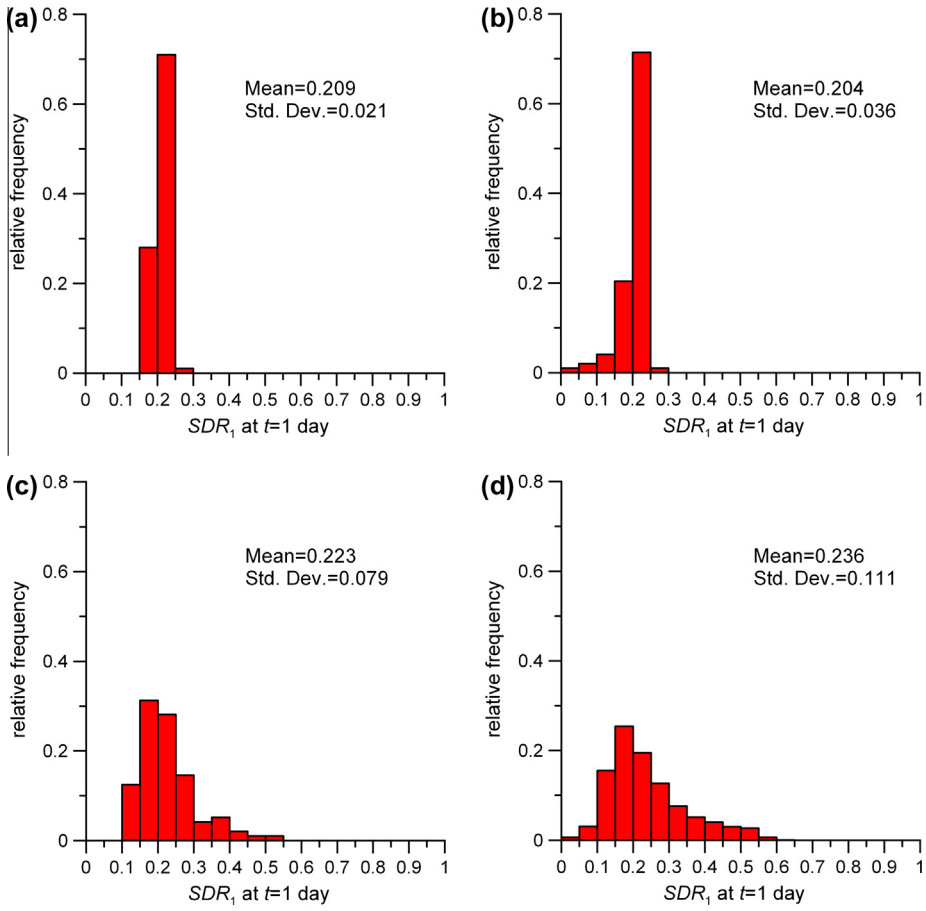

Fig. 11. Histograms of the *SDR* at $t = 1$ day for an unconfined aquifer with random variables of (a) K_h, (b) K_1, (c) K_v and (d) K_h, K_1 and K_v.

t = 10 h. The absolute value of the hydraulic head is equal to the drawdown from the pumping. This figure shows that the drawdown cone extends over the range of 300 m $\leqslant y \leqslant$ 700 m, which is within the reach of the weirs in the Doyleston Drain.

3.7. Uncertainty in SDR prediction

The sensitivity analysis is performed to examine the response of *SDR* to the changes of hydraulic parameters. Fig. 9 shows the temporal normalized sensitivity coefficients of the *SDR* evaluated by Eq. (31) to the changes of K_h, K_1, and S_s for a confined aquifer, K_h, K_1, S_s, K_v and S_y for an unconfined aquifer and K_h, K_1, S_s, K_v and K' for a leaky aquifer. The boundary effect of stream 2 is excluded by setting W_x = 10 km (i.e., ω_x = 200). For the case of the confined aquifer, the *SDR* at t = 0.02 day is most sensitive to the changes of the three parameters and the normalized sensitivities of K_h and S_s are relatively high as compared to the normalized sensitivity of K_1 shown in Fig. 9(a). In addition, the sensitivity curves of K_h and S_s are symmetrical in shape to the horizontal axis but have slightly different magnitudes, indicating that these two parameters are highly correlated (Yeh and Chen, 2007). For the case of the unconfined aquifer, the *SDR* is sensitive to the change of S_s before the very early time of t = 0.2 day and insensitive after the time. The *SDR* is sensitive to the changes of K_h, K_1 and K_v at the flat period and K_h, K_1 and S_y after the flat period. For the case of the leaky aquifer, the steady-state *SDR* after t = 0.2 day is sensitive to the changes of K_h, K_v, K_1 and K'. The curve of the sensitivity of S_s has a similar pattern to that for the case of the unconfined aquifer.

The Monte Carlo simulation is then used to assess uncertainty in the *SDR* prediction which is relatively sensitive to the changes of those parameters. For the case of the confined aquifer, the histograms of the *SDR* at t = 0.02 day are constructed by regarding S_s in Fig. 10(a), K_h in Fig. 10(b), K_1 in Fig. 10(c) and S_s, K_h and K_1 in Fig. 10(d) as random variables. The mean and standard deviation (Std. Dev.) of the *SDR* predictions for each histogram are shown in each panel. The variability in K_1 (Std. Dev. = 0.078) leads to the larger level of the uncertainty in the *SDR* predictions than those in S_s and K_h (Std. Dev. = 0.025 and 0.036, respectively). The uncertainty in the *SDR* predictions increases when considering the variabilities in S_s, K_h and K_1 (Std. Dev. = 0.090). Moreover, the variability in K_1 results in the left-skewed frequency distributions shown in Fig. 10c and d. This is because stream 1 becomes a constant head boundary when the realizations of K_1 are close to or larger than K_h and the predicted *SDR* for these realizations are near 0.42.

For the case of the unconfined aquifer, the histograms of the *SDR* at t = 1 day are constructed by regarding K_h in Fig. 11(a), K_1 in Fig. 11(b), K_v in Fig. 11(c) and K_h, K_1 and K_v in Fig. 11(d) as random variables. The S_s is considered as a deterministic value because of insensitivity at t = 1 day shown in Fig. 9(b). The variability in K_v (Std. Dev. = 0.079) leads to the larger level of the uncertainty in the *SDR* predictions than those in K_h and K_1 (Std. Dev. = 0.021 and 0.036, respectively). The variability in K_v produces the right-skewed frequency distributions in Fig. 11c and d because the aquifer provides most of water to the well extraction when the ratio of K_v/K_h goes large (Huang et al., 2012a). Furthermore, the histograms of the *SDR* at t = 30 day are constructed by regarding K_h in Fig. 12(a), K_1 in Fig. 12(b), S_y in Fig. 12(c) and K_h, K_1 and S_y in Fig. 12(d) as random variables. The S_s is also considered as a deterministic value. It is interesting to note that the variability in S_y results in the smaller level of the uncertainty in the model's outputs

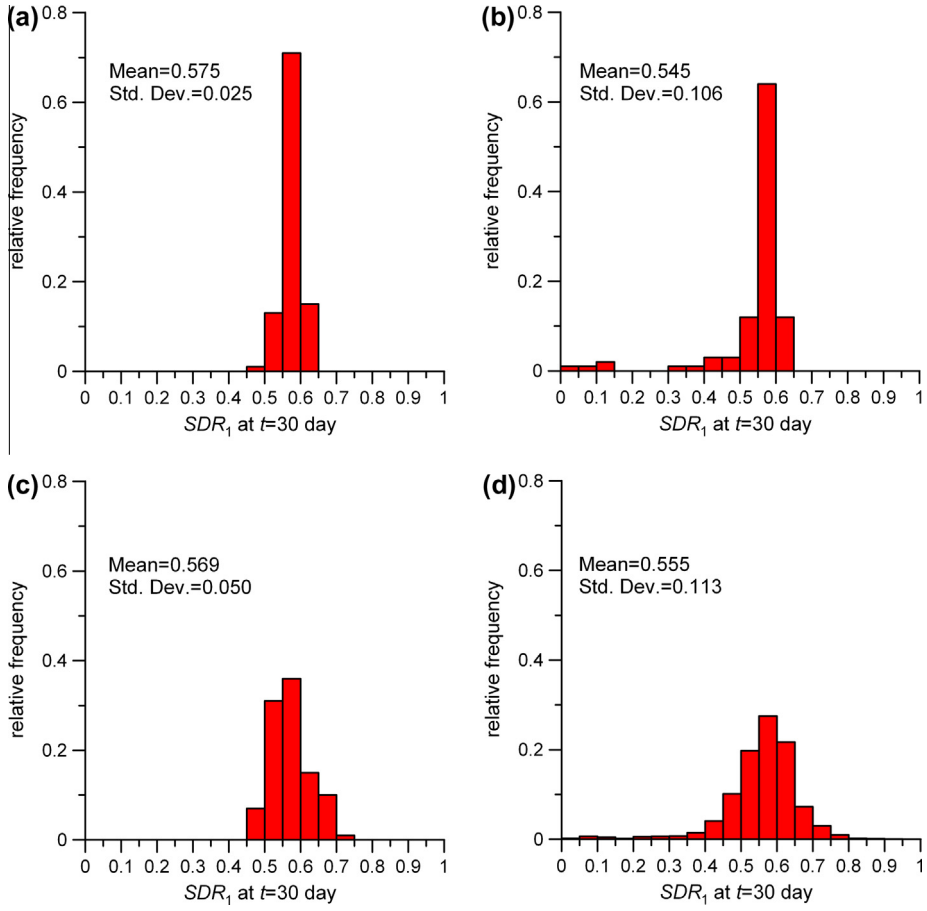

Fig. 12. Histograms of the *SDR* at t = 30 day for an unconfined aquifer with random variables of (a) K_h, (b) K_1, (c) S_y and (d) K_h, K_1 and S_y.

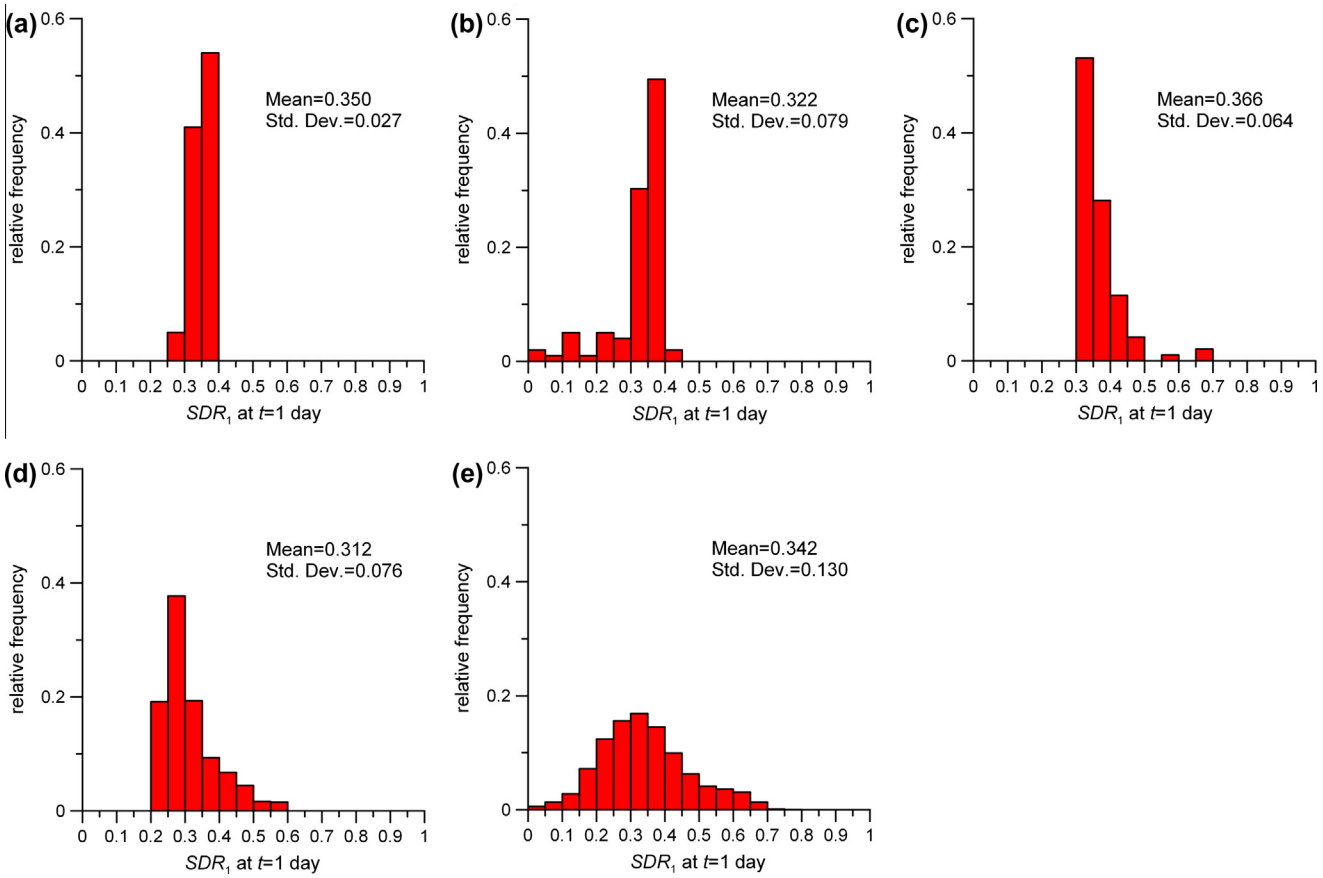

Fig. 13. Histograms of the *SDR* at $t = 1$ day for a leaky aquifer with random variables of (a) K_h, (b) K_1, (c) K_v, (d) K' and (e) K_h, K_1, K_v and K'.

than that in K_1 despite S_y is the most sensitive parameter at $t = 30$ day in Fig. 9(b).

For the case of the leaky aquifer, the histograms of the steady-state *SDR* at $t = 1$ day are constructed by regarding K_h in Fig. 13(a), K_1 in Fig. 13(b), K_v in Fig. 13(c), K' in Fig. 13(d) and K_h, K_1, K_v and K' in Fig. 13(e) as random variables. The S_s is also considered deterministic due to insensitivity at $t = 1$ day demonstrated in Fig. 9(c). The variability in K_1 (Std. Dev. = 0.079) leads to the greater level of the uncertainty in the *SDR* predictions than those in K_h, K_v and K' (Std. Dev. = 0.027, 0.064 and 0.076, respectively). The frequency distribution shown in Fig. 13(c) has a right skew because the vertical flow vanishes and the predicted *SDR* is 0.267 as discussed in Section 3.5. The variability in K' produces the right-skewed frequency distribution in Fig. 13(d) since the aquitard is very permeable when the realizations of K' are close to or larger than K_v, and the predicted *SDR* for these realizations are near 0.211. The pumped aquifer seems to contact directly with the upper aquifer in which the hydraulic head maintains constant. It is worth noting that the distribution in Fig. 13(e) tends to be normal because of the combination of the left-skewed frequency distribution due to the variability in K_1 and right-skewed frequency distributions due to the variabilities in K_v and K'.

4. Concluding remarks

A general analytical solution is developed for describing the temporal distribution of *SDR* induced by a fully-penetrating vertical well in an aquifers bounded by two parallel streams. A general top boundary condition is employed for the applications to confined, unconfined and leaky aquifers. Both streams with low-permeability streambeds are treated as the Robin boundary condition. The Laplace-domain head solution is derived using the double-integral transform and Laplace transform. The Laplace-domain *SDR* solution are obtained based on Darcy's law and the head solution. The time-domain *SDR* solution for the confined aquifer is developed analytically after applying the inverse Laplace transform. The time-domain *SDR* solutions for the leaky and unconfined aquifers are developed by taking Padé approximation and the inverse Laplace transform. The time-domain *SDR* solutions are expressed in terms of a simple series expanded by eigenvalues, which can be determined by a root-searching algorithm such as Newton's method. An analytical expression of the initial guesses is developed for the determination of the eigenvalues. The time-domain solutions give accurate predictions of *SDR* for the confined, leaky, and unconfined aquifers. The solution is applicable to an aquifer bounded either by two parallel streams or by a stream and a no-flow boundary. The temporal distribution of the *SDR* predicted by the time-domain solution for the confined aquifer agrees well with that taken from a field *SDR* experiment conducted by Hunt et al. (2001). The uncertainty in the *SDR* predictions for the aquifers is assessed by performing the sensitivity analysis and Monte Carlo simulation. With the aid of the time-domain solutions, the major conclusions can be drawn below:

1. For an unconfined aquifer, the gravity drainage rate increases with time toward a certain value, then maintains that value over a certain period, and finally decreases toward zero. The temporal *SDR* therefore has a flat stage in the intermediate period.
2. For a leaky aquifer, the leakage rate increases with time and then reaches its steady-state value which could be equal to or less than unity.

3. When $\kappa < 10$, neglecting the vertical flow component effect underestimates the *SDR* prediction for a leaky aquifer. The leakage should be imposed as the boundary condition at the top of the aquifer. When $\kappa \geqslant 10$, the vertical flow is negligible and the leakage can be treated as a source term in a 2-D flow governing equation.
4. The temporal *SDR* for a leaky aquifer is close to that for a confined one when $\kappa' \leqslant 10^{-4}$. The aquitard can thus be treated as an impermeable material, and the leaky aquifer behaves as a confined one.
5. For a confined aquifer, the *SDR* is sensitive to the changes of K_h, K_1 and S_s. For an unconfined aquifer, the *SDR* is sensitive to the changes of K_h, K_v and K_1 at a flat period and K_h, K_1 and S_y after the period. For a leaky aquifer, the steady-state *SDR* is sensitive to the changes of K_h, K_v, K_1 and K'.
6. The variability in K_1 results in a left-skewed frequency distribution of the *SDR* because stream 1 becomes a constant-head boundary.
7. The variability in K_v for unconfined and leaky aquifers leads to the right-skewed frequency distributions of the *SDR* because the vertical flow vanishes.
8. The variability in K' for a leaky aquifer produces the right-skewed frequency distributions of the *SDR* because the aquitard is as permeable as the pumped aquifer.

Acknowledgements

This study was partly supported by the Taiwan National Science Council under the Grants NSC 101-2221-E-009-105-MY2 and NSC 102-2221-E-009-072-MY2. The authors would like to thank the associate editor and the reviewer Dr. Nicholas Dudley Ward for his valuable and constructive comments.

Appendix A:. Double-integral transform

Latinopoulos (1985) presented a double-integral transform with various kernel functions corresponding to arbitrary two of the Dirichlet, no-flow and Robin boundaries. The double-integral transform with the kernel function corresponding to two Robin boundaries in x direction and two no-flow boundaries in y direction, in our notation, (Latinopoulos, 1985, aquifer type 4 in Table I, p. 298) is expressed as

$$H(\alpha_i,\beta_j) = \Im\{h(x,y)\} = \int_0^{\omega_y}\int_0^{\omega_x} h(x_D,y_D)K_e(\alpha_i,x_D)\cos(\beta_j y_D)dx_D dy_D \quad (A.1)$$

where $K_e(\alpha_i, x_D)$ has been defined by Eq. (10b), and α_i and β_j are the roots of Eq. (11) and $\sin(\omega_y\beta_j) = 0$, respectively. Applying the transform to the second-order differential terms $\partial^2 h_D/\partial x_D^2 + \partial^2 h_D/\partial y_D^2$ in Eq. (9a) and the integration by parts twice along with the boundary conditions, Eqs. (9c)–(9e), results in

$$\Im\left\{\frac{\partial^2 h_D}{\partial x_D^2}+\frac{\partial^2 h_D}{\partial y_D^2}\right\} = -(\alpha_i^2+\beta_j^2)H(\alpha_i,\beta_j) \quad (A.2)$$

The formula for the inverse double-integral transform is

$$h_D(x_D,y_D) = \Im^{-1}\{H(\alpha_i,\beta_j)\} = \frac{1}{\omega_y}\sum_{i=1}^{\infty}H(\alpha_i,0)K_e(\alpha_i,x_D) + \frac{2}{\omega_y}\sum_{j=1}^{\infty}\sum_{i=1}^{\infty}H(\alpha_i,\beta_j)K_e(\alpha_i,x_D)\cos(\beta_j y_D) \quad (A.3)$$

where $H(\alpha_i, \beta_j)$ herein represents the solution of Eq. (10a) with two boundary conditions, Eqs. (12a) and (12b).

References

Asadi-Aghbolaghi, M., Seyyedian, H., 2010. An analytical solution for groundwater flow to a vertical well in a triangle-shaped aquifer. J. Hydrol. 393 (3–4), 341–348. http://dx.doi.org/10.1016/j.jhydrol.2010.08.034.

Butler, J.J., Zlotnik, B.A., Tsou, M.S., 2001. Drawdown and stream depletion produced by pumping in the vicinity of a partially penetrating stream. Ground Water 39 (5), 651–659.

Butler, J.J., Zhan, X., Zlotnik, V.A., 2007. Pumping-induced drawdown and stream depletion in a leaky aquifer system. Ground Water 45 (2), 178–186. http://dx.doi.org/10.1111/j.1745-6584.2006.00272.x.

Chen, X., Yin, Y., 2004. Semianalytical solutions for stream depletion in partially penetrating streams. Ground Water 42 (1), 92–96.

Crump, K.S., 1976. Numerical inversion of Laplace transforms using a Fourier series approximation. J. ACM 23, 89–96.

Fox, G.A., DuChateau, P., Durnford, D.S., 2002. Analytical model for aquifer response incorporating distributed stream leakage. Ground Water 40 (4), 378–384.

Freeze, R.A., Cherry, J.A., 1979. Groundwater. Prentice-Hall, New Jersey.

Gerald, C.F., Wheatley, P.O., 1994. Applied Numerical Analysis, fifth ed. Addison-Wesley, New Jersey.

Glover, R.E., Balmer, G.G., 1954. River depletion resulting from pumping a well near a river. Trans. Am. Geophys. Union 35 (3), 468–470.

Hantush, M.S., 1965. Wells near streams with semi-pervious beds. J. Geophys. Res. 70 (12), 2829–2838.

Huang, Y.C., Yeh, H.D., 2007. The use of sensitivity analysis in on-line aquifer parameter estimation. J. Hydrol. 335 (3–4), 406–418. http://dx.doi.org/10.1016/j.jhydrol.12.007.

Huang, C.S., Chen, Y.L., Yeh, H.D., 2011. A general analytical solution for flow to a single horizontal well by Fourier and Laplace transforms. Adv. Water Resour. 34 (5), 640–648. http://dx.doi.org/10.1016/j.advwatres.2011.02.015.

Huang, C.S., Tsou, P.R., Yeh, H.D., 2012a. An analytical solution for a radial collector well near a stream with a low-permeability streambed. J. Hydrol. 446, 48–58. http://dx.doi.org/10.1016/j.jhydrol.2012.04.028.

Huang, C.S., Yeh, H.D., Chang, C.H., 2012b. A general analytical solution for groundwater fluctuations due to dual tide in long but narrow islands. Water Resour. Res. 48 (5), W05508. http://dx.doi.org/10.1029/2011WR011211.

Hunt, B., 1999. Unsteady stream depletion from ground water pumping. Ground Water 37 (1), 98–102.

Hunt, B., 2003. Unsteady stream depletion when pumping from semiconfined aquifer. J. Hydrol. Eng. 8 (1), 12–19. http://dx.doi.org/10.1061/(ASCE)1084-0699(2003)8:1(12).

Hunt, B., 2008. Stream depletion for streams and aquifers with finite widths. J. Hydrol. Eng. 13 (2), 80–89. http://dx.doi.org/10.1061/(ASCE)1084-0699(2008)13:2(80).

Hunt, B., 2009. Stream depletion in a two-layer leaky aquifer system. J. Hydrol. Eng. 14 (9), 895–903. http://dx.doi.org/10.1061/(ASCE)HE.1943-5584.0000063.

Hunt, B., Weir, J., Clausen, B., 2001. A stream depletion field experiment. Ground Water 39 (2), 283–289.

Intaraprasong, T., Zhan, H., 2009. A general framework of stream–aquifer interaction caused by variable stream stages. J. Hydrol. 373 (1–2), 112–121. http://dx.doi.org/10.1016/j.jhydrol.2009.04.016.

Jacob, C.E., 1950. Engineering Hydraulics. John Wiley & Sons, New York.

Latinopoulos, P., 1985. Analytical solutions for periodic well recharge in rectangular aquifers with third-kind boundary conditions. J. Hydrol. 77, 293–306.

Miller, C.D., Durnford, D., Halstead, M.R., Altenhofen, J., Flory, V., 2007. Stream depletion in alluvial valleys using the SDF semianalytical model. Ground Water 45 (4), 506–514. http://dx.doi.org/10.1111/j.1745-6584.2007.00311.x.

Neuman, S.P., 1972. Theory of flow in unconfined aquifers considering delayed response of the water table. Water Resour. Res. 8 (4), 1031–1045.

Sedghi, M.M., Samani, N., Sleep, B., 2009. Three-dimensional semi-analytical solution to groundwater flow in confined and unconfined wedge-shape aquifers. Adv. Water Resour. 32 (6), 925–935. http://dx.doi.org/10.1016/j.advwatres.2009.03.004.

Singh, S.K., 2009. Flow depletion induced by pumping well from stream perpendicularly intersecting impermeable/recharge boundary. J. Irrig. Drain. Eng. – ASCE 135 (4), 499–504, http://dx.doi.org/10.1061/(ASCE)IR.1943-4774.0000095.

Sophocleous, M., Koussis, A., Martin, J.L., Perkins, S.P., 1995. Evaluation of simplified stream–aquifer depletion models for water rights administration. Ground Water 33 (4), 579–588.

Sun, D., Zhan, H., 2006. Flow to a horizontal well in an aquitard–aquifer system. J. Hydrol. 321 (1–4), 364–376. http://dx.doi.org/10.1016/j.jhydrol.2005.08.008.

Sun, D., Zhan, H., 2007. Pumping induced depletion from two streams. Adv. Water Resour. 30 (4), 1016–1026. http://dx.doi.org/10.1016/j.advwatres.2006.09.001.

Swamee, P.K., Mishra, G.C., Chahar, B.R., 2000. Solution for a stream depletion problem. J. Irrig. Drain. Eng. – ASCE 126 (2), 125–126.

Teo, H.T., Jeng, D.S., Seymour, B.R., Barry, D.A., Li, L., 2003. A new analytical solution for water table fluctuations in coastal aquifers with sloping beaches. Adv. Water Resour. 26 (12), 1239–1247. http://dx.doi.org/10.1016/j.advwatres.2003.08.004.

Theis, C.V., 1941. The effect of a well on the flow of a nearby stream. EOS Trans. Am. Geophys. Union 22, 734–738.

Todd, D.K., Mays, L.W., 2005. Groundwater Hydrology, third ed. John Wiley & Sons, New York.

Tsou, P.R., Feng, Z.Y., Yeh, H.D., Huang, C.S., 2010. Stream depletion rate with horizontal or slanted wells in confined aquifers near a stream. Hydrol. Earth Syst. Sci. 14 (8), 1477–1485. http://dx.doi.org/10.5194/hessd-7-2347-2010.

Ward, N.D., Lough, H., 2011. Stream depletion from pumping a semiconfined aquifer in a two-layer leaky aquifer system. J. Hydrol. Eng. 16 (11), 955–959. http://dx.doi.org/10.1061/(ASCE)HE.1943-5584.0000382.

Yeh, H.D., Chen, Y.J., 2007. Determination of skin and aquifer parameters for a slug test with wellbore-skin effect. J. Hydrol. 342, 283–294. http://dx.doi.org/10.1016/j.jhydrol.2007.05.029.

Yeh, H.D., Chang, Y.C., Zlotnik, V.A., 2008. Stream depletion rate and volume of flow in wedge-shape aquifers. J. Hydrol. 349 (3–4), 501–511. http://dx.doi.org/10.1016/j.jhydrol.2007.11.025.

Yeh, H.D., Huang, C.S., Chang, Y.C., Jeng, D.S., 2010. An analytical solution for tidal fluctuations in unconfined aquifers with a vertical beach. Water Resour. Res. 46 (10), W10535. http://dx.doi.org/10.1029/2009WR008746.

Zhan, H., Park, E., 2003. Horizontal well hydraulics in leaky aquifers. J. Hydrol. 281 (1–2), 129–146. http://dx.doi.org/10.1016/S0022-1694(03)00205-1.

Zhan, H., Zlotnik, V.A., 2002. Ground water flow to horizontal and slanted wells in unconfined aquifers. Water Resour. Res. 38 (7), 1108. http://dx.doi.org/10.1029/2001WR000401.

Zlotnik, V.A., Huang, H., 1999. Effect of shallow penetration and streambed sediments on aquifer response to stream stage fluctuations (analytical model). Ground Water 37 (4), 599–605.

Zlotnik, V.A., Tartakovsky, M., 2008. Stream depletion by groundwater pumping in leaky aquifers. J. Hydrol. Eng. 13 (2), 43–50. http://dx.doi.org/10.1061/(ASCE)1084-0699(2008)13:2(43).